NECROTIC CELL DEATH: A NOVEL OUTCOME OF BHPI-HYPERACTIVATION OF THE ANTICIPATORY UNFOLDED PROTEIN RESPONSE

BY

MARA R LIVEZEY

DISSERTATION

Submitted in partial fulfillment of the requirements
for the degree of Doctor of Philosophy in Biochemistry
in the Graduate College of the
University of Illinois at Urbana-Champaign, 2018

Urbana, Illinois

Doctoral Committee:

Professor David J. Shapiro, Chair
Professor Benita Katzenellenbogen
Assistant Professor Erik Procko
Professor Emad Tajkhorshid

ABSTRACT

Of the roughly 1 in 8 women that develop breast cancer in their lifetimes, 70% will have estrogen receptor α positive (ERα$^+$) cancer. The standard of care for these cancers is endocrine therapy, including aromatase inhibitors and selective estrogen receptor modulators and degraders (SERMs and SERDs), that either block the production of estrogen or competitively inhibit the binding of estrogen to ERα. These small molecule antiestrogens work by inhibiting the pro-proliferative actions of estrogen but after years of treatment, many cancers recur as resistant tumors. Recently, we discovered a non-competitive modulator of ERα that works in a strikingly different way. BHPI acts through ERα to hyperactivate a lethal anticipatory unfolded protein response (UPR), hijacking a normally protective and pro-proliferative action of estrogen and ERα. We have found that BHPI effectively inhibits proliferation of and kills breast cancer cells expressing constitutive and antiestrogen resistant mutations, ERαY537S and ERαD538G, that are common in metastatic breast cancer and upregulate the UPR. Surprisingly, BHPI does not kill cancer cells through classical UPR activated, CHOP-mediated, caspase-dependent apoptosis, but rather through necrosis initiated by ATP depletion. This death pathway includes rapid swelling of ERα$^+$ cancer cells and release of arachidonic acid, and is downstream of calcium release from the endoplasmic reticulum (EnR). Interestingly, preliminary data suggests that necrotic products released from cells treated with BHPI may act as markers of inflammation that activate immune cells. Strong and sustained activation of the anticipatory UPR leading to necrotic cell death and inflammation may represent a new strategy to target ERα$^+$ cancers.

ACKNOWLEDGEMENTS

First and foremost, thank you to Dr. David J. Shapiro for your support and guidance over the past four years. You were an excellent mentor and allowed me the independence to grow and pursue areas of science that I was most passionate about. A big thank you to Dr. Mao, who has been an immeasurable asset in my work. Thanks also to the entire Shapiro lab team whom I had the pleasure to work with: Ji, Xiaobin, Liqun, Darjan, Lawrence, and Santanu, your insight was most appreciated. A special thank you to Rui Huang, your contribution to this work cannot be overstated and it was an honor to work with and mentor you.

I would also like to thank Dr. Laura Furge, who first trained me as an undergraduate researcher and inspired me to pursue a doctoral degree.

Electron microscopy was performed in the Frederick Seitz Materials Research Laboratory Central Research Facilities and flow cytometry was done at the Roy J. Carver Biotechnology Center, University of Illinois. We thank Michael Lambrecht for synthesizing BHPI. This research was supported by grants DOD BCRP W81XWH-13, NIH RO1 DK071909, and the E. Howe Scholar Award (DJS), and by an NSF Graduate Research Fellowship under DGE-1144245 (ML).

The work presented here is dedicated to my loving and supportive family. Thank you for encouraging my curiosity and for nurturing the scientist that has always lived within me.

TABLE OF CONTENTS

CHAPTER 1: INTRODUCTION

This work contains previously published material.[1]

Abstract

Cells react to a variety of stresses, including accumulation of unfolded or misfolded protein, by activating the endoplasmic reticulum (EnR) stress sensor, the unfolded protein response (UPR). The UPR is highly conserved and plays a key role in the maintenance of protein folding quality control and homeostasis. In contrast to the classical reactive mode of UPR activation, recent studies describe a hormone-activated anticipatory UPR. In this pathway, mitogenic hormones such as estrogen (E_2), epidermal growth factor (EGF), and vascular endothelial growth factor (VEGF) rapidly activate the UPR in anticipation of a future need for increased protein folding capacity upon cell proliferation. Here, I focus on this recently unveiled pathway of E_2-estrogen receptor α (ERα) action. Notably, rapid activation of the anticipatory UPR pathway is essential for subsequent activation of the E_2-ERα regulated transcription program. Moreover, activation of the UPR at diagnosis is a powerful prognostic marker in ERα positive breast cancer. Lethal ERα-dependent hyperactivation of the anticipatory UPR represents a promising therapeutic approach exploited by a novel small molecule ERα biomodulator, BHPI, and may be effective against recently identified ERαY537S and ERαD538G mutations common in metastatic breast cancer. However, the death pathway activated by BHPI in ERα positive cancer cells remained to be described.

[1] Livezey, M. et al. Frontiers in Endocrinology, 2018. Reference 154.

Introduction

The endoplasmic reticulum (EnR) plays a key role in the synthesis, folding, and transport of proteins and is important in lipid synthesis.[1,2] Maintenance of protein folding and lipid homeostasis is critical for cell proliferation and viability. The unfolded protein response (UPR) is an EnR stress-response pathway that senses and responds to diverse stimuli, including changes in EnR luminal calcium, redox status, nutrient availability, lipid bilayer composition, and accumulation of unfolded or misfolded protein.[3,4] The UPR consists of three arms, IRE1α, ATF6α, and PERK, that together decrease the flux of new protein into the EnR while simultaneously increasing production of molecular chaperones to help fold unfolded or misfolded proteins. IRE1α and PERK are activated upon oligomerization and autophosphorylation. ATF6α is activated and transported to the Golgi apparatus, where it is cleaved by S1P and S2P proteases, although the mechanism of activation in the EnR is still unclear. There is increasing evidence that all three arms of the UPR can be activated in more than one way. For example, some of the earliest work suggested that the molecular chaperone, BiP, blocked oligomerization and activation of IRE1α and PERK through direct binding to their luminal domains.[2] Upon accumulation of unfolded or misfolded proteins, BiP would be competed away, allowing activation of these UPR arms. Similarly, it is thought that upon depletion of EnR calcium, calcium-dependent molecular chaperones, such as BiP, fall off IRE1α and PERK, and other unfolded or misfolded proteins. This would allow IRE1α and PERK to oligomerize and activate the UPR.[5] Additional experiments and elucidation of the crystal structure of the luminal domain of IRE1α showed that independent of BiP binding, IRE1α can directly bind and be activated by peptides via an MHC-like structural domain.[2] Interestingly, recent work has also suggested that IRE1α and PERK may sense and be activated by changes in lipid

content of the EnR membrane, independent of accumulation of unfolded protein or depletion of calcium in the EnR.[6]

Activation of the non-canonical RNase IRE1α (inositol-requiring enzyme 1α) results in alternative splicing of the transcription factor XBP1, leading to the production of spliced-XBP1 (sp-XBP1) and upregulation of molecular chaperones.[7] ATF6α (activating transcription factor 6α) is translocated to the Golgi apparatus where it is cleaved by proteases to produce the transcription factor p50-ATF6α that also upregulates chaperone production.[8] Lastly, activated PERK (protein kinase RNA-like endoplasmic reticulum kinase) phosphorylates eIF2α, resulting in transient inhibition of most protein synthesis while promoting translation and production of selective proteins including ATF4, CHOP, $p58^{IPK}$, and GADD34.[9] When UPR stress is mild, the chaperone $p58^{IPK}$ binds to and inhibits PERK, and GADD34 dephosphorylates eIF2α. Working together, $p58^{IPK}$ and GADD34 reverse PERK activation and restore protein synthesis.

Classically, the UPR is activated in response to EnR stress. Several years ago, it was shown that progenitors of immunoglobulin-producing B cells activate the UPR before initiating antibody production.[10,11] This pathway, which is activated in absence of unfolded protein, was named the anticipatory UPR by Peter Walter and David Ron,[2] but it was not studied extensively. We, and others, recently showed that diverse steroid and peptide hormones including estrogen (17β-estradiol, E_2), progesterone (P_4), epidermal growth factor (EGF), and vascular endothelial growth factor (VEGF), and probably the insect hormone ecdysone (Ec), activate an anticipatory UPR pathway to prepare cells for the increased protein folding that accompanies cell proliferation.[12–16] Notably, the steps between hormone-receptor complexes and activation of the three arms of the UPR have largely been identified.[12–14]

The proliferative and anti-apoptotic advantage of overexpressing or activating hormone receptors, such as EGF receptor (EGFR) or estrogen receptor α (ERα), has long been appreciated in cancer biology.[17–20] However, hormone activation of the anticipatory UPR has only recently become a focus of cancer research and exploited as a therapeutic target. Here, we focus on the role of E_2-ERα activation of the anticipatory UPR and a promising preclinical drug candidate, BHPI, which leverages this novel action of ERα in order to block proliferation of and kill most ERα positive breast cancer cells.

Activation of the anticipatory UPR by mitogenic hormones

Steroid and peptide hormones exert their effects through binding and modulating their specific receptors.[20,21] Using E_2-ERα as an example, when hormone receptors bind their ligand, they dimerize and are recruited to specific DNA response elements (Figure 1). E_2-ERα then modulates the activity of thousands of genes either through direct binding to DNA, or by tethering of E_2-ERα to other transcription factors.[22–24] The genomic actions of E_2-ERα are important for the pro-proliferation properties of E_2 in ERα positive breast cancer cells and while rapidly initiated, play out over hours or days.

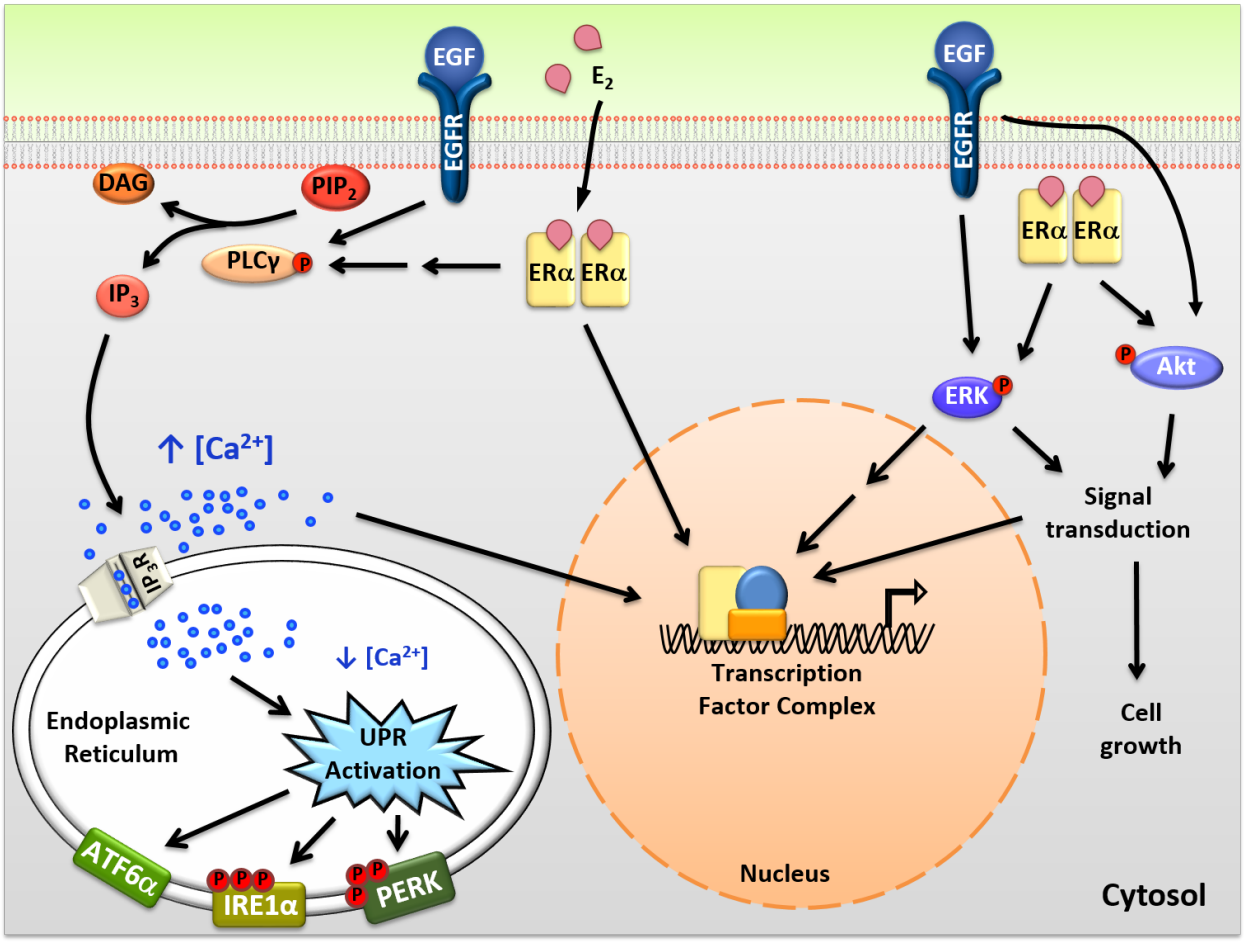

Figure 1. Intracellular actions of mitogenic hormones. Estrogen (E_2) and epidermal growth factor (EGF) act on their respective receptors, ERα and EGFR, to initiate crosstalk between extranuclear signaling pathways and their genomic programs. ERα indirectly and EGFR directly activate phospholipase C γ (PLCγ), resulting in cleavage of PIP_2 to DAG (diacylglycerol) and IP_3 (inositol triphosphate). IP_3 then binds to IP_3 receptors (IP_3Rs) in the endoplasmic reticulum (EnR) membrane, causing moderate efflux of calcium from the lumen of the EnR into the cell body. This calcium signal activates all three arms of the unfolded protein response (UPR) and acts as an authorizing signal for E_2-ERα and EGF-EGFR modulation of gene expression and cell proliferation. In parallel, E_2-ERα and EGF-EGFR modulate additional extranuclear signal transduction pathways, including activation of ERK and Akt signaling. Activation of these pathways is also important for subsequent cell proliferation and crosstalks with the E_2-ERα and EGF-EGFR genomic programs.

In addition to classical genomic actions, E_2-ERα exerts rapid extranuclear actions important for activating signal transduction pathways (Figure 1). These pathways are important for diverse actions of E_2-ERα, crosstalk with the genomic program, and are rapidly activated and often play

out over minutes to hours.[25,26] Of these pathways, activation of the anticipatory UPR is the most recently described (Figure 1).[14] Upon binding of E_2 to ERα at the plasma membrane, there is rapid activation of phospholipase C γ (PLCγ), resulting in cleavage of its substrate PIP_2 to IP_3 (inositol triphosphate) and DAG (diacylglycerol). The IP_3 then binds to and opens IP_3 receptor (IP_3R) calcium channels in the membrane of the EnR, allowing efflux of calcium out of the lumen of the EnR into the cell body. The modest decrease in EnR calcium caused by E_2 treatment of ERα positive cancer cells weakly activates the UPR, resulting in upregulation of molecular chaperones along with minimal and very transient inhibition of protein synthesis. By knockdown of UPR components, or blocking calcium release from the EnR, we showed that increased intracellular calcium from activation of the anticipatory UPR is critical for subsequent E_2-ERα-mediated modulation of gene expression and cell proliferation.[14]

In diverse cancers, mild UPR activation is protective and helps cancers proliferate, induce angiogenesis, and overcome hypoxia and toxic stress from chemotherapies.[27,28] Using microarray and outcome data from approximately 1,000 patient breast cancers, we demonstrated the significance of this pathway in ERα positive breast cancer. Increased expression of a UPR gene index consisting of UPR-components and UPR-induced chaperones strongly correlated with reduced time to recurrence, subsequent resistance to tamoxifen, and reduced survival.[14] The close correlation between the extent of activation of the UPR gene index and activation of E_2-ERα regulated genes is consistent with ERα playing a major role in the elevated expression of the UPR gene index.[29] Moreover, in triple negative breast cancer in which ERα is absent, the IRE1/XBP1 axis plays a central role in tumorigenicity and progression, and the extent of activation of an XBP1 gene index is correlated with reduced patient survival.[30,31] Taken together, this suggests that ERα-mediated activation of the anticipatory UPR likely plays an important role in early survival of

breast cancers. At later times when therapeutic stress is added to nutritional deprivation and hypoxia, activation of the classical reactive UPR makes an important contribution to tumor survival.[28,32–34]

Because of the protective nature of the UPR in cancer, drugs that target components of the UPR are in pre-clinical development, in clinical trials, and have been approved.[30,31,35] Most commonly, these drugs inhibit key components of the UPR such as PERK, IRE1α RNase, or the downstream chaperone BiP/GRP78. Unfortunately, due to lack of drug specificity, these drugs may have toxic effects in tissues with a large secretory burden, such as pancreas.

UPR hyperactivation as a tool to selectively target ERα positive breast cancer

Recently, we described a novel small molecule biomodulator, BHPI, that selectively targets ERα positive cancer cells.[15,29,36] BHPI (3,3-bis(4-hydroxyphenyl)-7-methyl-1,3,dihydro-2H-indol-2-one) is a bis-phenylated oxoindol. In a limited structure-activity-relationship (SAR) study, addition of methyl groups to both phenyl rings significantly disrupted activity of BHPI.[29] We demonstrated specificity by testing over 30 ERα positive and negative cell lines and showed that BHPI only inhibits proliferation of or kills cells that express ERα.[29] Additionally, in the isogenic human breast cell lines MCF10A (ERα negative) and MCF10A$_{ER\ IN9}$ (ERα positive), we showed that BHPI was only effective in the cells expressing ERα, and was ineffective when ERα was knocked back down in MCF10A$_{ER\ IN9}$ cells. Demonstrating that BHPI physically interacts with ERα, BHPI shifts the tryptophan emission spectrum of ERα and protects peptides in the ERα ligand binding domain from protease digestion. Furthermore, BHPI inhibits recruitment of ERα to E_2-ERα regulated promoters (Figure 2). However, BHPI is not a competitive inhibitor, as it does not compete with radiolabeled E_2 for the ligand binding pocket and is equally effective in the

presence and absence of estrogen.[29] Rather than inhibiting a component of the UPR, BHPI takes advantage of the already moderately-elevated UPR in cancer cells by hyperactivating the anticipatory UPR (Figure 2). BHPI therefore hijacks the normal protective actions of ERα activation of the UPR in order to push UPR activation into the lethal range. This is the first small molecule to modulate the action of a hormone receptor in this way.

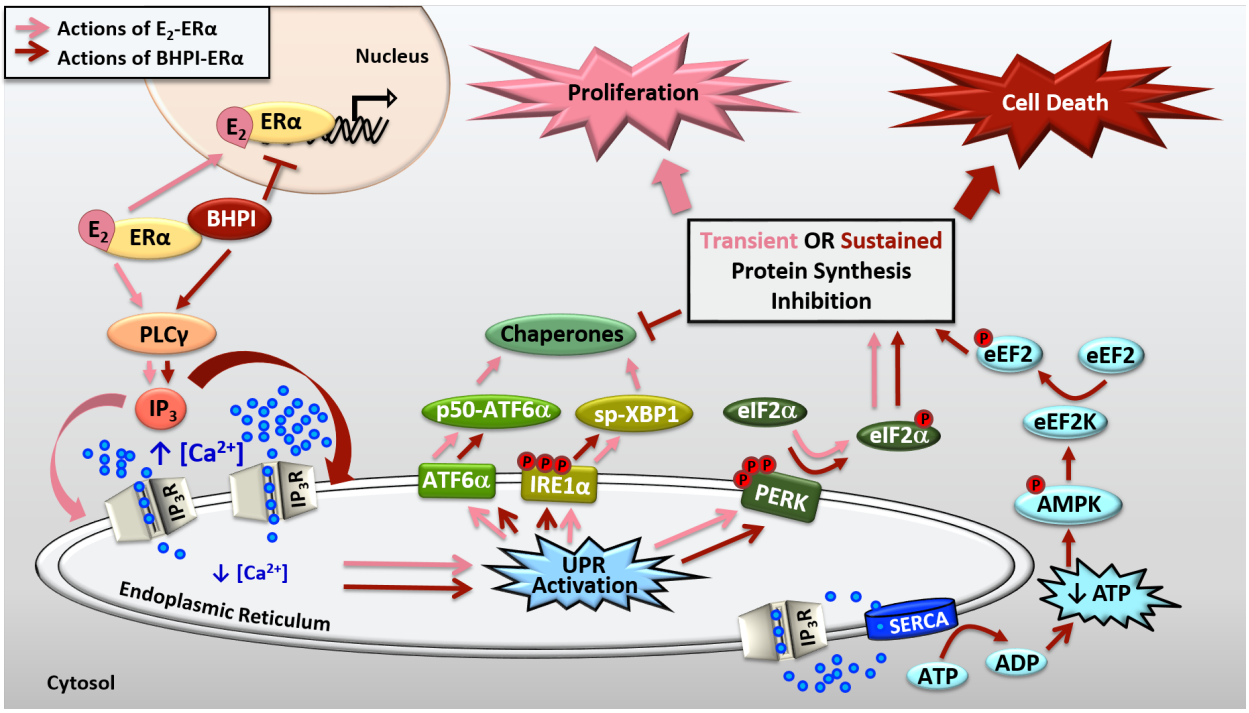

Figure 2. Activation of the anticipatory unfolded protein response by ERα. E_2-ERα and constitutively active ERα mutants activate a mild and protective anticipatory unfolded protein response (UPR) and the non-competitive biomodulator BHPI binds ERα and induces hyperactivation of this pathway leading to cell death. ERα indirectly activates phospholipase C γ (PLCγ), resulting in cleavage of PIP_2 to DAG (diacylglycerol) and IP_3 (inositol triphosphate). E_2-ERα and constitutively active ERα mutants cause moderate IP_3 production whereas BHPI causes significantly more production of IP_3. The IP_3 then binds to IP_3 receptors (IP_3Rs) in the endoplasmic reticulum (EnR) membrane, causing efflux of calcium from the lumen of the EnR into the cell body. E_2-ERα and constitutively active ERα mutants cause moderate and transient release of calcium, resulting in weak and transient activation of all three arms of the unfolded protein response (UPR). Weak UPR activation results in very mild and transient inhibition of protein synthesis, production of molecular chaperones, and is critical for subsequent cell proliferation. BHPI-ERα induced hyperactivation of the UPR causes robust and sustained release

Figure 2 (cont.) of calcium from the EnR. This leads to robust PERK activation and rapid, sustained, and near-quantitative inhibition of protein synthesis. Although BHPI causes upregulation of chaperone mRNA, no protein is made, and the UPR-activating signal is never resolved. In an effort to re-establish cellular calcium homeostasis, ATP-dependent SERCA pumps in the EnR actively transport calcium back into the lumen of the EnR but since IP_3Rs remain open, an ATP-depleting futile cycle ensues. Decreased cellular ATP and increased AMP activate AMPK, which along with calcium, activates Ca^{2+}/calmodulin-dependent kinase, eukaryotic elongation factor 2 kinase (CAMKIII/eEF2K). eEF2K then phosphorylates eEF2 (eukaryotic elongation factor 2), causing inhibition of protein synthesis at elongation. Ultimately, BHPI-ERα induced hyperactivation of the anticipatory UPR causes death of ERα positive endometrial and breast cancer cells.

We showed that BHPI blocks proliferation of ovarian cancer cells and kills most ERα positive breast and endometrial cancer cells.[15,29,36] Compared to E_2, BHPI causes increased production of IP_3 in cancer cell lines.[29,36] This increased production of IP_3 hyperactivates the UPR through sustained opening of IP_3R calcium channels in the EnR, resulting in robust and sustained calcium release from the lumen of the EnR into the cell body (Figure 2). While E_2 causes mild and transient inhibition of protein synthesis, BHPI causes a rapid, sustained, and near-quantitative inhibition of protein synthesis in ERα positive breast and endometrial cancer cells. Surprisingly, BHPI also causes rapid depletion of intracellular ATP. Disruption of cytosolic calcium homeostasis can be toxic, specifically, high levels of calcium can lead to cell death.[37–39] To restore intracellular calcium homeostasis after opening of IP_3Rs, ATP-dependent SERCA pumps in the EnR membrane pump calcium back into the EnR lumen, but because IP_3Rs remain open, the calcium leaks back out. This creates a futile cycle of calcium leakage and pumping that depletes intracellular ATP. Additionally, ATP depletion from prolonged SERCA pump activity results in increased levels of cellular AMP that activates the metabolic sensor AMPK. AMPK activation together with high levels of cytosolic calcium activate the Ca^{2+}/calmodulin-dependent kinase, eukaryotic elongation factor 2 kinase (CAMKIII/eEF2K). Activated eEF2K then phosphorylates eukaryotic elongation factor 2 (eEF2), which inhibits protein synthesis at a second site (Figure 2). Therefore, although

BHPI increases the mRNA levels of chaperones such as BiP and $p58^{IPK}$, no protein is made, leading to un-resolvable cytotoxic activation of the UPR. While other activators of the classical reactive UPR share similarities to BHPI's mechanism of action, such as disruption of EnR calcium homeostasis and inhibition of protein synthesis,[1,2] BHPI is unique in its ability to cause ATP depletion in cancer cells.

In ovarian cancer, a common mechanism for resistance to the taxane paclitaxel and other chemotherapy agents is overexpression of ATP-dependent efflux pumps, especially Multidrug Resistance Protein 1 (MDR1)/P-glycoprotein/ABCB1. Despite intensive efforts, effective and non-toxic MDR1 inhibitors have remained elusive. Due to its ability to deplete intracellular ATP, BHPI inhibited ATP-dependent MDR1-mediated drug efflux and restored sensitivity of multidrug resistant breast and ovarian cancer cells to killing by therapeutically relevant concentrations of several anticancer drugs.[36] Using multidrug resistant OVCAR-3 cells, BHPI was tested in an orthotopic ovarian cancer xenograft model. Although paclitaxel was ineffective against these tumors, BHPI alone strongly reduced tumor growth. Notably, tumors were undetectable in mice treated with BHPI plus paclitaxel. After the combination therapy, plasma levels of the widely used cancer biomarker, CA125, were at least several hundred-fold lower than in mice with control tumors. Moreover, CA125 levels progressively declined to undetectable in all mice treated with the combination therapy.[36]

The standard of care for ERα positive breast cancer is endocrine therapy, including aromatase inhibitors that block E_2 production, and tamoxifen and fulvestrant/ICI that compete with E_2 for binding to ERα. Unfortunately, many tumors that were initially responsive recur after years of treatment. Moreover, there is selection and outgrowth of endocrine therapy resistant tumors expressing ERα mutations in about one-third of patients with advanced metastatic breast cancer,

most commonly ERαY537S and ERαD538G.[40–42] Structural and biophysical studies suggest that estrogen receptors containing these mutations are stabilized in the active conformation and have lower affinity for antiestrogens such as OHT.[43] Additionally, a growing body of clinical evidence suggests that mutations in this ligand binding domain hotspot confer partial resistance to endocrine therapies.[40–42,44] Strikingly, patients whose tumors express ERαY537S or ERαD538G have on average 12 and 6 months shorter survival, respectively, than patients whose tumors express wild-type ERα.[45] Because of the resistance to endocrine therapies observed in cancers expressing ERαY537S and ERαD538G, development of better selective estrogen receptor modulators and degraders (SERMs and SERDs) has been a focus in targeting these cancers.[46–49] It was not known whether BHPI could effectively target these cells.

Hyperactivation of the anticipatory UPR and cell death

While the initial steps of BHPI-hyperactivation of the anticipatory UPR are well described, the consequences for cell fate were unclear, especially in cancer cells expressing the ERαY537S or ERαD538G mutations. Most small molecules that target the classical reactive UPR kill cells by activating caspase-dependent apoptosis.[50–52] This pathway is characterized by UPR activation inducing production of the pro-apoptotic effector, CHOP, that downregulates Bcl2 to initiate apoptosis.[53] Disruption of calcium homeostasis and mitochondrial dysregulation are also associated with UPR-induced apoptosis. Apoptosis is characterized by formation of the apoptosome, autoactivation and cleavage of caspase-9, the subsequent cascade of caspase activation including caspase-3, and breakdown of cellular components.[54] Morphologically, apoptosis is characterized by cell shrinking, DNA condensation, and formation of apoptotic bodies.

Many of the small molecules that activate the classical UPR also induce autophagy. Autophagy is often a protective mechanism used to cope with cellular stress but when left unchecked, can result in cell death, especially in cells that are deficient in the apoptotic machinery. Autophagic cell death is characterized by increased production of LC3-II and other markers such as Beclin-1, as well as visualization of LC3-II puncta in the initial stages of autophagosome formation. Changes in cell morphology include formation of many double-membraned autophagosomes filled with cellular debris.[33,55]

Lastly, although less well-understood and less common, cells can die through necrosis. Unlike programmed cell death, where cells go through a series of defined steps, necrosis is generally thought of as accidental death. Necrosis is characterized by calcium dysregulation, cell swelling, loss of membrane integrity, and eventual release of cytosolic contents into the surrounding area.[38,56] Recent studies have suggested that necroptosis, a subset of necrotic cell death, may represent the first example of programmed necrosis.

The fate of cells that have experienced strong and sustained activation of the anticipatory UPR following BHPI treatment was unknown. Uncovering the death pathway activated by BHPI is not only important to understanding its action as a pre-clinical anti-cancer drug. Although this type of death has not been described in normal physiology, understanding this pathway might shed light on how accidentally-prolonged activation of the anticipatory UPR under normal conditions, such as in immunoglobulin-producing B cells,[10,11] might lead to cell death.

Conclusion

Studies of the pro-proliferative effects of mitogenic hormones and their respective receptors have long focused on their actions on genomic programs and on extranuclear signal transduction

pathways. Activation of the anticipatory UPR is an emerging, very rapid action of many mitogenic hormones that authorizes subsequent gene expression and cell proliferation. Important for targeting hormone receptor positive breast cancers is the finding that they exhibit elevated UPR activation. This UPR activation can be exploited by small molecules that hyperactivate the pathway, pushing UPR activation into the lethal range. As a first-in-class small molecule, BHPI is a model for investigating hyperactivation of the anticipatory UPR as a promising strategy for killing ERα positive breast cancer cells. A similar approach is also likely viable for breast cancers that overexpress other hormone receptors that activate the anticipatory UPR, such as progesterone receptor, or EGFR family members. However, agents that hyperactivate the anticipatory UPR through these receptors have yet to be identified. Thus, the anticipatory UPR is a key pathway for development of new anti-cancer drugs that can help overcome resistance to current therapies.

CHAPTER 2: MATERIALS AND METHODS

Cell culture and reagents. Cell culture medium and conditions were as previously described.[57] T47D, MCF7, ECC-1, MDA MB-231, HeLa, ES2, HEK 293T, and MCF10A cells were from ATCC. BT-474 cells were provided by Dr. R. Schiff, $MCF10A_{ER\ IN9}$ cells were provided by Dr. B.H. Park, and TamR cells were provided by Dr. D. McDonnell. T47D-ERαY537S (TYS) and T47D-ERαD538G (TDG) were made as we recently described.[15] Cells were grown in the following conditions: T47D (MEM, 10% FBS), ERαY537S and ERαD538G (MEM, 10% charcoal:dextran-treated (CD)-FBS), MCF-7 (MEM, 5% FBS), ECC-1 (RPMI, 5% FBS), MDA MB-231 (MEM, 5% FBS), HeLa (RPMI1640, 10% FBS), ES2 (McCoy's 5a, 10% FBS), HEK 293T (DMEM, 10% FBS), MCF10A (2% CD-FBS, 20ng/ml EGF), BT-474 (RPMI1640, 10% FBS), and TamR (DMEM/F12 +NEAA +100 nM z-OHT, 8% FBS). Reagents used were: ICI 182,780 (Tocris Biosciences, UK), trans-ISRIB, SKF 96365, and BAPTA-AM (Cayman Chemical, MI), fulvestrant/ICI 182,780 (Tocris Bioscience, MN), bortezomib, 7-Cl-O-Nec-1, and GSK872 (EMD Millipore, MA), niflumic acid, quinacrine dihydrochloride, and Z-VAD-FMK (Santa Cruz Biotechnology, TX), ^{3}H-arachidonic acid and ^{35}S-methionine (Perkin Elmer, MA), all other reagents were from Sigma Aldrich (MO).

Generation of ERαY537S and ERαD538G cell lines. Our protocol was loosely based on previous work.[58] Two guide sequences (Supplementary Fig. S1) were cloned into pSpCas9(BB)-2A-Puro(PX459) (Addgene, MA). An HDR template with mutations was cloned into pUC18, and linearized before transfection. Two plasmids with guide sequences and the HDR template carrying either the ERαY537S or ERαD538G mutation were co-transfected into T47D cells. After 3-day

selection in 2.5 μg/ml puromycin, followed by 3 weeks of E_2-free growth, colonies were transferred to a 24-well plate. Clones were genotyped at the DNA and mRNA levels using PCR and restriction enzyme digestion. Sequencing confirmed selected clones. Oligonucleotide sequences and additional details are in Supplementary Methods.

MTS cell proliferation assay. Cell proliferation assays in 2D culture were performed as described.[29] Briefly, 2,000 cells/well were incubated with treatment for 4 days with one medium change after 2 days. After 4 days, 20 μl of CellTiter 96 Aqueous One Solution (Promega, WI) was added to each well and absorbance measured.

Quantitative proliferation assays in 3D culture. Quantitative assays of colonies in soft agar were as in[59] with minor modifications. Briefly, 2,000 cells in 60 μl 0.4% agar were plated in 96-well plates above 50 μl 0.6% agar. Cells were grown for 5 days with one medium change, treated with AlamarBlue (Fisher, NH) and fluorescence measured.

Alamar Blue Cell Proliferation Assay

Cells were plated at the indicated density into 96-well plates. The next day, the medium was changed to one containing the indicated treatment. The medium was changed again after 2 days and proliferation assayed after a total of 4 days. Cell number was measured with Alamar Blue (ThermoFisher, MA) and compared to a standard curve of cell number versus fluorescence.

Western Blotting

Western blotting was carried out as previously described.[14,57] The following primary antibodies were used: PARP (Cell Signaling Technology (CST) #9532), Bcl2 (CST #4223), LC3A/B (CST #4108), Beclin-1 (CST #3738), CHOP (CST #2895), p-p70S6K (T389) (CST # 9234), ERα (CST # 8644), HMGB1 (Novus Biologicals, 2F6), PLCγ (CST #5690), and β-actin (Sigma, A1978). Antibodies were probed with HRP-conjugated secondary antibodies (ThermoFisher) and imaged with the ECL2 detection kit (Fisher Scientific, MA) using a PhosphorImager.

Trypan Blue Exclusion and Cell Swelling

Cell viability or cell diameter after treatment with BHPI or other compounds were measured using a Countess II cell counter (ThermoFisher). 300 000 cells/well were plated in 6-well plates. The next day, vehicle or treatment was added for the indicated time. Cells were then harvested and concentrated to 2-5 million cells/ml before addition of trypan blue immediately before counting for cell viability or diameter.

Lentiviral Production

Constructs for packaging vectors pCI-VSVG (#1733) and psPAX2 (#12260), pHIV-Luciferase (#21375), and pCDH-Bcl2 (#46971) were from Addgene (MA). Lentiviral packaging vectors were co-transfected with either luciferase or Bcl2 into HEK 293T cells with Lipofectamine 3000 (Invitrogen, CA). The next day, medium was changed. Virus was harvested 24 hours later and used to infect TYS cells for 48 hours before analysis of trypan blue uptake or western blotting.

Flow Cytometry

300 000 cells/well were plated in 6-well plates. The next day, vehicle or treatment was added for the indicated time. Cells were then harvested, washed with PBS, and stained with the Dead Cell Apoptosis Kit (ThermoFisher). After staining, cells were measured on a BD LSR II (BD Biosceinces, NJ) and data was analyzed using FCS Express (DeNovo, CA).

Transmission Electron Microscopy

The cell pellet was fixed in a Karnovsky's Fixative in phosphate-buffered 2% glutaraldeyde and 2.5 % paraformaldehyde. Microwave fixation was used with this primary fixative and the tissue was then washed in Sorenson's phosphate buffer without additives. Microwave fixation was also used with the secondary 2% osmium tetroxide fixative, followed by the addition of 3% potassium ferricyanide for 30 minutes. After washing with water, saturated uranyl acetate was added for enbloc staining. The tissue was dehydrated with a series containing increasing concentrations of ethanol. Acetonitrile was used as the transition fluid between ethanol and the epoxy. Infiltration series was done with an epoxy mixture using the epon substitute Lx112. The resulting blocks were polymerized at 90 °C overnight, trimmed and ultrathin sectioned with diamond knives. Sections were stained with uranyl acetate and lead citrate and examined or photographed with a Hitachi H600 Transmission Electron Microscope at 75KV.

Lactate Dehydrogenase (LDH) Release

LDH release into the medium was measured according to the CytoTox-ONE Homogeneous Membrane Integrity Assay protocol (Promega, WI).

siRNA Knockdown of ERα and PLCγ

Knockdown of ERα or PLCγ was performed using DharmaFECT1 transfection reagent and 100 nM ON-TARGETplus non-targeting pool or SMARTpool for ERα (ESR1) or PLCγ (PLCG1) (Dharmacon, CO). T47D or TYS cells were treated with non-coding or coding siRNA for 16 hours and the medium was replaced thereafter. To further reduce the levels of ERα, 24 hours after changing the medium, 1 μM of ICI was added to the samples that received ERα siRNA and vehicle was added to the untreated and non-coding samples. Cell swelling was assayed after an additional 24 hours. Trypan blue uptake in TYS cells was measured 48 hours following transfection.

Protein Synthesis

Rates of protein synthesis were evaluated by measuring ^{35}S-methionine incorporation into newly synthesized protein as described previously.[29] Briefly, cells were incubated with treatment for the indicated time and 3 μCi ^{35}S-methionine was added for the last 30 min of treatment. Cells were washed with PBS and lysed in RIPA buffer. Lysates were spun and supernatants were pipetted onto Whatman 540 filter-paper discs and subsequently washed 3X each with 10% TCA, then 5% TCA, and air dried. Protein was solubilized and counts were measured to determine percent protein synthesis inhibition.

^{3}H-Arachidonic Acid Release from Cell Membranes

Phospholipase cleavage of arachidonic acid (AA) from membranes was determined by measuring release of ^{3}H-AA into medium. To allow overnight incorporation into membranes, 100 000 cells/well were plated in a 24-well plate and incubated overnight in medium containing 0.1% fatty acid-free BSA and ^{3}H-AA to a final concentration of 0.1 μCi/ml. The next day, the medium was

removed, and cells were washed 4X with incubation medium (25 mM HEPES pH 7.2, 150 mM NaCl, 5 mM KCl, 5.5 mM dextrose, 0.8 mM $MgSO_4$, 1 mM $CaCl_2$, 0.1% BSA). Incubation medium containing the treatment was added and cells were incubated at 37 °C for 45 minutes. Medium was collected, and cells were lysed in 0.1 M NaOH. ^3H counts for the medium and cell lysate were determined and AA release was normalized to total incorporated label.

BHPI-Stimulated Prostaglandin Release

Cells were plated to 70% confluency; the next day, the medium was changed to MEM + 0.1% BSA with treatment. 24 hours later, the medium was collected, spun down, and the supernatant was collected and evaporated before resuspension and analysis following the Prostaglandin Screening Kit protocol (Cayman Chemical).

ATP Measurement

ATP depletion was performed as previously described[29] and ATP levels were measured according to the ATPlite Luminescence Assay Kit protocol (Perkin Elmer).

mRNA Induction and Migration of THP-1 Cells

T47D or TYS cells were grown to 70-80% confluency. Cells were washed once with PBS, and the medium was replaced with serum-free medium containing the indicated treatment. After 24 hours, the conditioned medium was taken, spun down to remove cell debris, and the supernatant was collected for further use. BHPI was added to the control conditioned medium after isolation. Raptinal-treated T47D or TYS cells were treated for 4 hours before washing the small molecule out to eliminate apoptotic effects on THP-1 cells. For mRNA experiments, THP-1 cells were

differentiated in 10 nM phorbol-12-myristate-13-acetate (PMA) for 3 days. The following day, medium was replaced. 24 hours later, conditioned medium was added to a final volume of 1:1 with normal culture medium and RNA was extracted after 6 hours.

To measure migration, THP-1 cells were spun down and resuspended in serum-free medium. 200,000 cells were plated in the upper well of a Boyden chamber in 100 µL volume. 400 µL of conditioned medium was added to the bottom of each well, and the cells were allowed to migrate for 4 hours. After 4 hours, migration was measured with the QCM Chemotaxis 5 µm 24-Well Cell Migration Assay Kit (Millipore).

CHAPTER 3: ANTIESTROGEN RESISTANT CELL LINES EXPRESSING ESTROGEN RECEPTOR α MUTATIONS UPREGULATE THE UNFOLDED PROTEIN RESPONSE AND ARE KILLED BY BHPI

This work contains previously published material.[2]

Abstract

Outgrowth of metastases expressing ERα mutations Y537S and D538G is common after endocrine therapy for estrogen receptor α (ERα) positive breast cancer. The effect of replacing wild type ERα in breast cancer cells with these mutations was unclear. We used the CRISPR-Cas9 genome editing system and homology directed repair to isolate and characterize 14 T47D cell lines in which ERαY537S or ERαD538G replace one or both wild-type ERα genes. In 2-dimensional, and in quantitative anchorage-independent 3-dimensional cell culture, ERαY537S and ERαD538G cells exhibited estrogen-independent growth. A progestin further increased their already substantial proliferation in micromolar 4-hydroxytamoxifen and fulvestrant/ICI 182,780 (ICI). Our recently described ERα biomodulator, BHPI, which hyperactivates the unfolded protein response (UPR), completely blocked proliferation. UPR-regulated proteins associated with tamoxifen resistance, including the oncogenic chaperone BiP/GRP78, were upregulated. ICI displayed a greater than 2-fold reduction in its ability to induce ERαY537S and ERαD538G degradation. Progestins, UPR activation and perhaps reduced ICI-stimulated ERα degradation likely contribute to antiestrogen resistance seen in ERαY537S and ERαD538G cells.

[2] Mao, C., et al. Scientific Reports, 2016. Data from Figures 3-6, 8(a,b), and 9 was obtained by Dr. Chengjian Mao. Reference 15.

Introduction

Endocrine therapy for estrogen receptor α (ERα) positive breast cancers employs aromatase inhibitors to block estrogen production and tamoxifen and fulvestrant/Faslodex/ICI 182,780 (ICI) that compete with estrogens for binding to ERα. For advanced metastatic breast cancer, selection and outgrowth of tumors resistant to endocrine therapy and expressing ERα mutations ERαY537S and ERαD538G is common.[40,41,44,60] There is compelling evidence these mutations are resistant to aromatase inhibitors.[40–42,44,60–62] While most evidence suggests they are also clinically resistant to tamoxifen and fulvestrant/ICI,[60,63,64] recent studies demonstrated increased prevalence of ERα mutations in breast cancers of patients treated with aromatase inhibitors, but not in patients treated with fulvestrant,[42] or tamoxifen.[61] These researchers question the association of ERα mutations with clinical resistance to fulvestrant and tamoxifen. In studies mostly using transfected ERα negative cells, the mutants were reported to be resistant to tamoxifen and ICI,[60] resistant to tamoxifen but sensitive to ICI[41] and sensitive to antiestrogen inhibition.[40,65] Previously described systems for analyzing the ERαY537S and ERαD538G mutations were not ideal. Cell lines derived from circulating tumor cells exhibit multiple genetic changes and lack a control cell line. Transfected ERα negative cell lines do not exhibit estrogen-ERα regulated proliferation and display a different ERα-regulated gene expression pattern than ERα positive breast cancer cells.[66] A better experimental model would compare cells expressing the ERα mutations and wild type ERα in a defined genetic background in an ERα positive breast cancer cell whose proliferation is stimulated by estrogen. We therefore used the CRISPR-Cas9 gene editing system to produce multiple cell lines in which one or both copies of the wild type ERα gene was replaced by ERαY537S or ERαD538G.

Although the most common application of the CRISPR-Cas9 system is targeted gene inactivation by non homologous end joining (NHEJ) to repair the Cas9 generated DNA break, when a homologous repair donor is present, a homology-directed repair process (HDR) can precisely insert a sequence containing the desired modification into the gene of interest. Because the frequency of HDR is usually extremely low,[67–71] the CRISPR-Cas9 system has rarely been used to successfully repair or insert specific mutations in both copies of endogenous genes in a cancer cell line. We used the CRISPR-Cas9 gene editing system to generate 50 clonal cell lines with one or both copies of endogenous wild-type ERα replaced with ERαY537S or ERαD538G.

Although progesterone reportedly plays a role in breast cancer progression,[72,73] a recent study concluded that when E_2 is present, progesterone enhances tamoxifen's effectiveness as an antiestrogen.[74] The effect of progestins in cells expressing ERα mutations had not been explored.

We showed that the estrogen, 17β-estradiol (E_2), acts through ERα to elicit extremely rapid and functionally important anticipatory activation of the endoplasmic reticulum stress sensor, the unfolded protein response (UPR).[14] Moreover, activation of a UPR gene index at diagnosis is a powerful prognostic indicator, tightly correlated with subsequent resistance to tamoxifen therapy.[14] This ERα-regulated UPR pathway is targeted by BHPI, our recently described noncompetitive ERα biomodulator. BHPI hyperactivates the UPR, converting it from cytoprotective to cytotoxic.[29,36] While BHPI is effective in tamoxifen-resistant breast cancer cells expressing wild type ERα, its effectiveness in cells expressing ERα mutations associated with metastases was unknown.

Here we describe the effects of OHT, ICI and BHPI on proliferation of the ERαY537S and ERαD538G cells in anchorage dependent and anchorage independent culture with and without a

progestin, and evaluate estrogen-independent and progestin-stimulated UPR activation and reduced ERα degradation as potential contributors to antiestrogen resistance.

Results

Using CRISPR-Cas9 to replace wild-type ERα with ERαY537S or ERαD538G.

Our strategy is illustrated in Figure 3. To facilitate identification of cells in which the mutant ERα fragment replaced the wild-type ERα fragment, we inserted AclI and SpeI sites into the HDR template.

We chose T47D cells because they contain 2 copies of the ERα gene and exhibit E_2 dependent growth.[75] Previous transfection studies suggested ERαY537S and ERαD538G cells grow without E_2.[40,41,44] We exploited this phenotype during outgrowth and selection of colonies of ERαY537S and ERαD538G cells.

Individual colonies were pulled, grown out, and genotyped. Genomic DNA spanning the HDR template was amplified and analyzed by digestion with AclI or SpeI (Figure 3). 50 of 65 clonal cell lines contained single or double gene replacements (Figure 4). Expression of the ERα mutations in mRNA was confirmed by synthesizing and digesting cDNA, followed by sequencing (Figure 3). We used ERαY537S-4 and ERαD538G-1 as representative clones, as their properties matched other ERαY537S and ERαD538G clones. Sequencing and Western blotting with N-terminal ERα antibody showed that NHEJ introduced diverse indels in the non-replaced copy of ERα (Figures 3 and 4). We therefore focused primarily on double replacement cell lines.

Western blotting to compare ERα levels in parental T47D cells to levels of ERαY537S and ERαD538G in single and double replacement cell lines showed some heterogeneity in expression

level of ERαY537S and ERαD538G. The ERα mutations were expressed at levels similar to or lower than wild-type ERα (Figure 4).

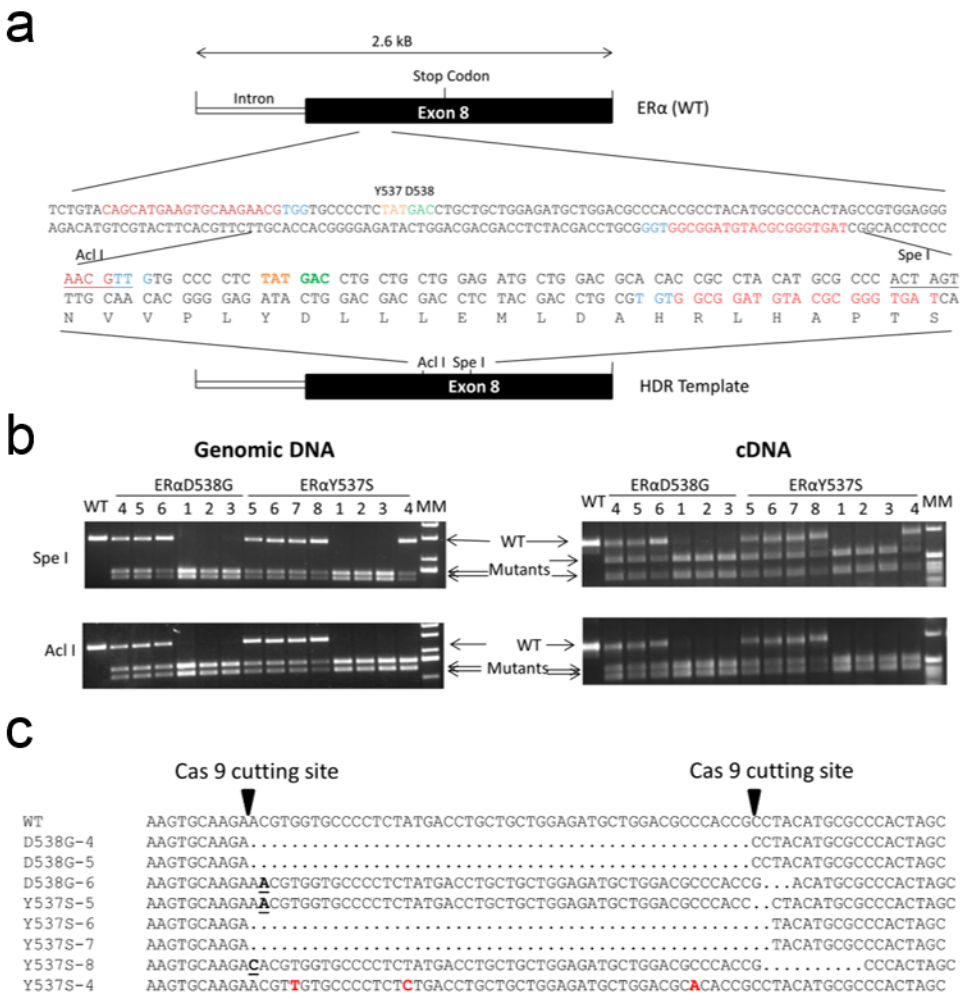

Figure 3. CRISPR-Cas9 replacement of wild-type ERα with ERαY537S and ERαD538G. (a) Design of the HDR template for gene replacement. The ERα genomic fragment containing part of intron 7 and exon 8 was amplified by PCR, sequenced and compared to database sequences. Blue nucleotides indicate the native or mutated PAM sequence. The single nucleotide changes do not alter the amino acid sequence of ERα or use rare codons. These changes will block cutting of the edited gene by Cas9. Guide sequences are in red. Underlined regions indicate single nt changes to generate AclI or SpeI sites that do not alter the amino acid sequence. The changes to yield the desired mutations were: ERαY537S: TAT to TCT (orange); ERαD538G: GAC to GGG (green). (b) Genotyping of cell lines: Analysis of genomic DNA and cDNA from clonal cell lines for restriction sites indicating gene replacement. Genomic DNA or cDNA generated from total RNA was used as template for PCR amplification with ERα specific primers. The PCR primers were outside the HDR template or corresponding mRNA region. PCR products from each clone

Figure 3 (cont.) were subjected to AclI or SpeI digestion. Digestion patterns after agarose gel electrophoresis and staining with ethidium bromide are shown for 14 randomly chosen clones, 8 from Y537S and 6 from D538G. (c) Identification of insertions and deletions (indels) in the non-replaced copy of ERα. The undigested (SpeI and AclI) DNA bands from cell lines in which one copy of wild-type ERα was replaced (single replacement) were purified by agarose gel electrophoresis and sequenced. For both guide sequences, the Cas9 cleavage site is noted. Inserted nucleotides are underlined and deletions are shown by dots. The sequence of all digested bands are as designed (not shown). In ERαY537S-4 one ERα gene is missing the SpeI site and sequencing confirmed the presence of the ERαY537S mutation and mutation of both PAM sequences. Therefore, we can confirm two distinct and independent events replaced both copies of wild-type ERα. This also suggests a homologous recombination event between the restriction site and the PAM sequence. Since sequencing the undigested SpeI ERαY537S-4 band confirmed the ERαY537S and PAM sequence mutations, one of the two homologous recombination events occurred in the 50 nucleotide region between the Y537S mutation and SpeI site. This is the only recombination event observed within 50 bp of the mutation site among all 50 clones (1 out of 130 possible recombination events [potentially 4 recombination events/double replacement]). Thus, using long 1.2 kb homologous arms likely increased the probability of HDR.

a

Summary of CRISPR-Cas9 Gene Replacement

	Both ERα Copies Replaced	One ERα Copy Replaced	False Positive
ERαY537S	9	23	14
ERαD538G	6	12	1
Total	15	35	15

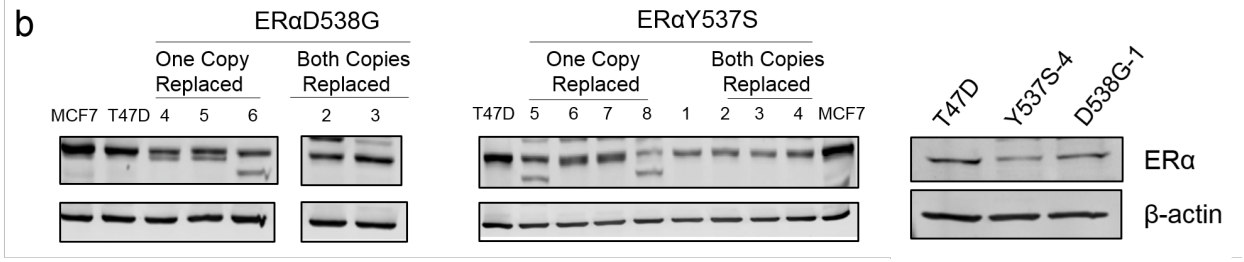

Figure 4. Summary of CRISPR-Cas9 gene replacement. (a) Table 1 summarizes data for all the clonal cell lines genotyped. Despite the low frequency of HDR for both the ERαY537S and ERαD538G mutations, almost half as many assayed cell lines had both copies of the wild-type ERα replaced with the mutation as cell lines that had one copy replaced. Although we did not observe a substantial growth advantage for the double replacement cell lines in standard cell culture, it remains possible that they exhibited a somewhat larger growth advantage during outgrowth of the clones. The reason for the small number of false positive cell lines in the

Figure 4 (cont.) ERαD538G experiments is unknown. (b) Western blot analysis of ERα expression. To ensure detection of deletions and truncations in the C-terminal region of ERα, we used an antibody recognizing epitopes in the N-terminal region of ERα. The Western blot shows that the pattern of ERα gene expression in the cell lines replacing one copy of the ERα gene matches that predicted from the DNA sequencing. For example: In Supplementary Figure S1c, clones ERαD538G-4 and ERαD538G-5 show a deletion of 17 amino acids and a reading frame shift after the deletion. This results in a protein, containing 588 amino acids with almost 60 amino acids after a reading frame shift. This protein's size is very close to the size of wild-type ERα as seen by two bands in the western (595 aa). For clones D538G-6, Y537S-5 and Y537S-8, a single nt insertion causes a reading frame shift and premature termination, resulting in truncation of the protein. For these 3 clones, this insertion results in a protein with 537 total amino acids seen as a second, lower molecular weight band than wild-type ERα. For clones Y537S-6 and Y537S-7, there are deletions and reading frame shifts, resulting in a protein containing 579 amino acids. On the gel, the ERα band is broad and blurry, suggesting two bands.

ERαY537S and ERαD538G cells exhibit E_2-independent growth and partial resistance to OHT and ICI.

Although the clonal cell lines were isolated and maintained without E_2, it was unknown whether E_2 further stimulates their growth. As expected, the parental T47D cells exhibited little growth without E_2 and dose-dependent increases in growth with E_2 (Figure 5a).[29] The ERαY537S-4 cells and the other ERαY537S cell lines were completely E_2-independent for growth. E_2 further stimulated the more modest E_2-independent proliferation of ERαD538G-1 and other ERαD538G cells (Figures 5a and 6).

We next performed dose response studies evaluating the effect of OHT and ICI on proliferation of the T47D, ERαY537S and ERαD538G cell lines. To facilitate comparisons, T47D and mutant cells were maintained in medium containing E_2. In T47D cells, OHT and ICI nearly abolished proliferation at a 50-1,000 fold molar excess over E_2 (Figure 5b,c). In contrast, the mutant cell lines, especially ERαY537S-4, exhibited some resistance (Figure 5b,c; blue bars). Additionally, while T47D cells displayed negligible growth in ICI, all seven ERαY537S and ERαD538G double replacement cell lines displayed at least some growth in ICI (Figure 6). In longer 8-day cultures,

compared to T47D cells, the mutant cells displayed increased proliferation in OHT and ICI (Figure 7).

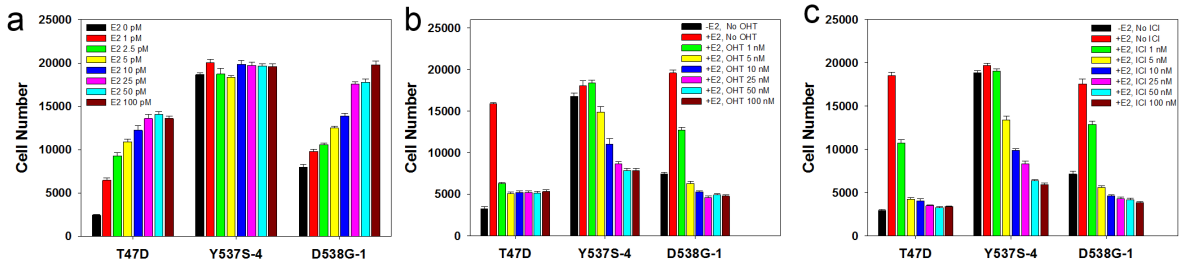

Figure 5. In standard anchorage-dependent 2D culture, ERαY537S-4 and ERαD538G-1 cells exhibit E_2-independent proliferation and partial resistance to OHT and ICI. (a) Dose-response study comparing the effects of increasing concentrations of E_2 on the proliferation of T47D, ERαY537S-4 and ERαD538G-1 cells. (b and c) Dose-response studies comparing the effects of increasing concentrations of OHT (b) and ICI (c) on the proliferation of T47D, ERαY537S-4 and ERαD538G-1 cells. Data is mean ± SEM (n=8).

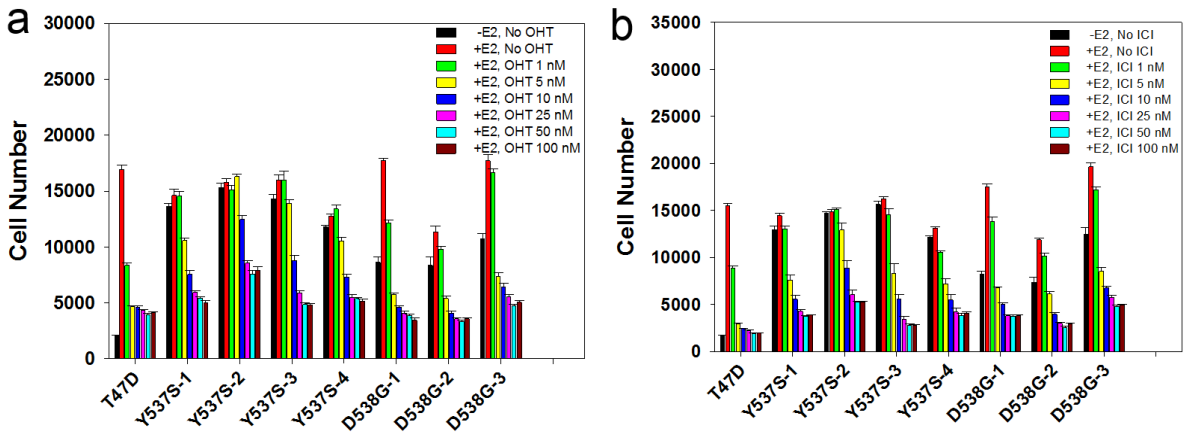

Figure 6. In standard 2D culture, additional ERαY537S and ERαD538G cells exhibit partial resistance to OHT and ICI. Dose-response studies comparing the effects of increasing concentrations of OHT (a) and ICI (b) on the proliferation of T47D and additional double replacement ERαY537S and ERαD538G cell lines. Data is mean ± SEM (n=8).

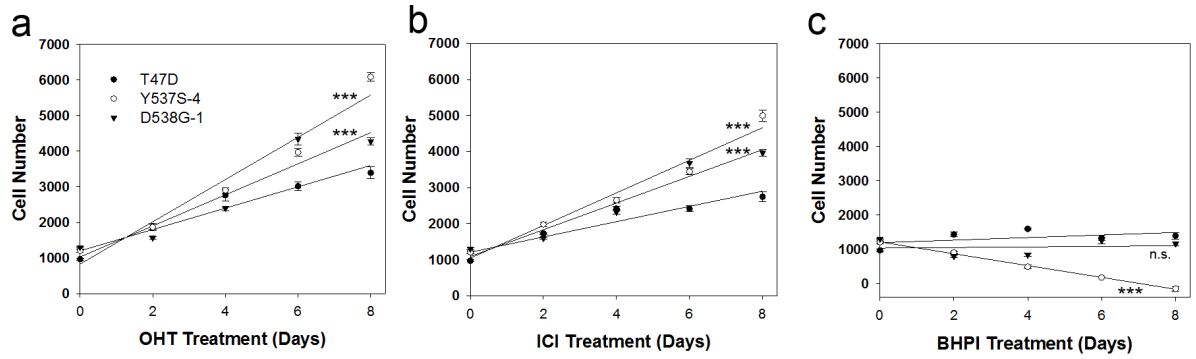

Figure 7. In longer-term 2D culture, ERαY537S-4 and ERαD538G-1 cells exhibit continued proliferation in the presence of ICI and OHT, but not with BHPI. 1,000 cells were seeded into each well of a 96-well plate. The next day (day 0), treatment was started. Medium with treatment was changed every two days. Data is mean ± SEM (n=8). Slopes of the lines were compared using the free online calculator (http://www.danielsoper.com/statcalc/calculator.aspx?id=103). ***: $p<0.001$. Statistics were calculated using all collected data (not mean values) comparing the slope of the T47D line to either ERαY537S-4 or ERαD538G-1. Slopes were calculated by linear regression and are as follows- OHT: T47D: 300 ± 22, ERαY537S-4: 593 ± 25, ERαD538G-1: 437 ± 28; ICI: T47D: 214 ± 17, ERαY537S-4: 441 ± 17, ERαD538G-1: 375 ± 18; BHPI: T47D: 37 ± 14, ERαY537S-4: -172 ± 7, ERαD538G-1: 9 ± 15.

BHPI blocks growth of ERαY537S and ERαD538G cells.

Since the ERαY537S and ERαD538G cell lines displayed partial resistance to OHT and ICI, we evaluated the ability of our recently described noncompetitive ERα biomodulator, BHPI, to inhibit proliferation of ERαY537S and ERαD538G cells.[29] At 25 nM, BHPI completely inhibited proliferation of T47D, ERαY537S-4 and ERαD538G-1 cells and the 14 characterized ERα mutant cell lines (Figures 8a and 9). In longer 8-day cultures, BHPI continued to completely block proliferation of T47D, ERαY537S-4 and ERαD538G-1 cells (Figure 7).

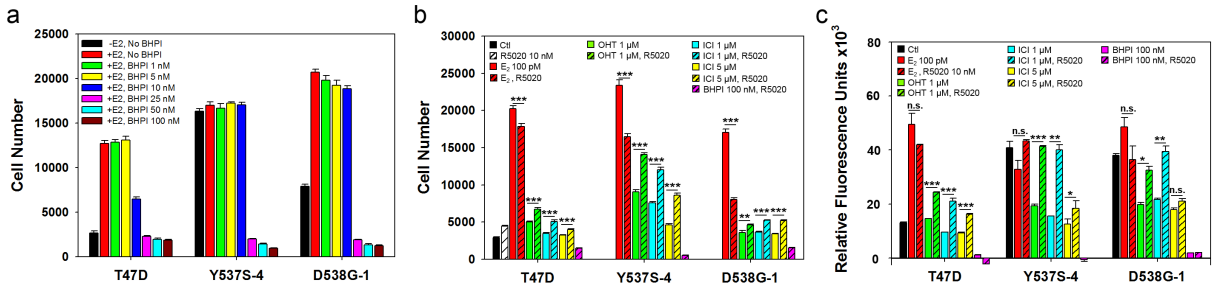

Figure 8. ERαY537S-4 and ERαD538G-1 cells show antiestrogen resistant growth in 2D and 3D culture, but are killed by BHPI. (a) Dose-response study of the effect of BHPI on the proliferation of T47D, ERαY537S-4 and ERαD538G-1 cells in standard anchorage-dependent 2D culture. (b) In 2D culture, R5020 reduces the ability of OHT and ICI to inhibit proliferation of ERαY537S-4 and ERαD538G-1 cells. (c) In 3D culture, ERαY537S-4 and ERαD538G-1 cells are highly antiestrogen resistant and resistance is robustly increased by R5020, but the cells are killed by BHPI. Conditions (a-c) as noted, with 100 pM E_2 unless otherwise stated. Data is mean ± SEM (n=8). For (b,c) *:p<0.05, **: p< 0.01, ***: p< 0.001 (by Student's T test) comparing treatment to treatment + R5020.

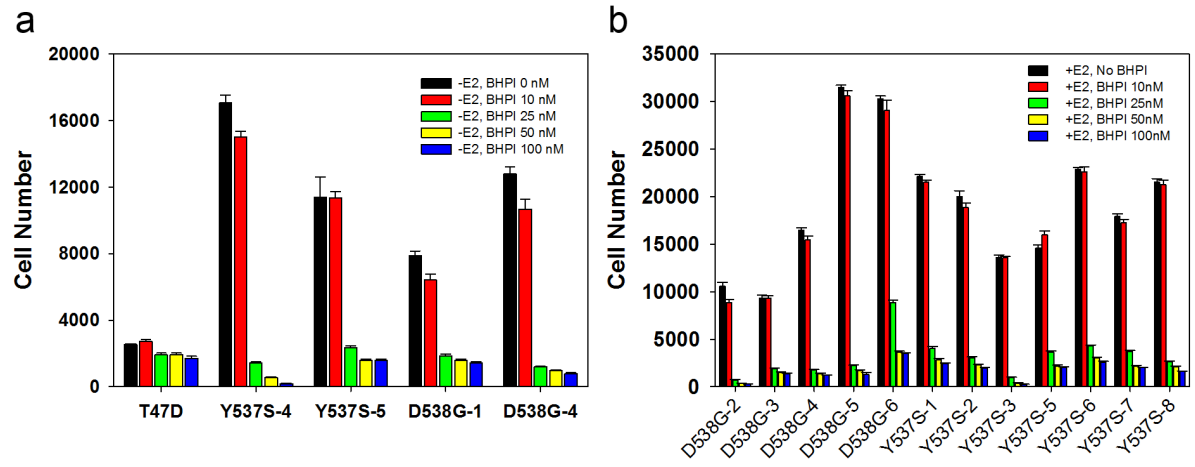

Figure 9. BHPI blocks proliferation and often kills ERαY537S and ERαD538G cells with or without added E_2. (a) Dose-response studies showing 25 nM BHPI is effective in inhibiting proliferation of ERαY537S and ERαD538G cells in the absence of E_2. (b) Dose-response studies showing all double and single gene replacement ERαY537S and ERαD538G cell lines are responsive to BHPI in the presence of E_2. Independent of the presence of ERα deletions in the non-replaced copy of the single replacement cell lines, or of the formation of ERα heterodimers, BHPI retains full effectiveness and blocks proliferation of every ERα mutant cell line characterized. Data is mean ± SEM (n=8).

ERαY537S and ERαD538G cells exhibit progesterone-stimulated antiestrogen-resistant, BHPI-sensitive, growth in anchorage-independent culture.

Although anchorage-independent growth in 3-dimensional (3D) culture is a hallmark of cancer, it has been difficult to study quantitatively. Modifying earlier methods,[59] we developed a protocol for quantitative assessment of cell proliferation in a more biologically relevant anchorage-independent 3D culture in soft agar.

We compared the effects of OHT (1 μM; 10,000 fold excess over E_2), ICI (1 and 5 μM), BHPI (100 nM) and the synthetic progestin R5020 (10 nM), on proliferation of ERαY537S-4 and ERαD538G-1 cells in anchorage-dependent 2D and anchorage-independent 3D culture. 5 μM OHT was not used because it exhibits nonspecific toxicity.[76–78] In standard 2D culture, the ERαY537S-4 cells exhibited reduced, but significant proliferation in OHT and ICI, which was increased by R5020. The ERαD538G-1 cells exhibited little proliferation in OHT and ICI, which increased slightly in R5020 (Figure 8b, compare open bars: no R5020, hatched bars: + R5020).

In quantitative 3D culture, ICI was more effective than OHT in blocking growth of T47D cells. Impressively, proliferation of the mutants in 1 μM OHT and ICI was >50% of control, a dramatic increase compared to 2D culture (Figure 8c). At 1 μM, ICI was no more effective than OHT in inhibiting proliferation of the mutants. Notably, in 3D culture, ERαY537S-4 and ERαD538G-1 cells grown in R5020 were completely resistant to growth inhibition by 1 μM OHT and ICI (Figure 8c).

In both 2D and 3D culture, BHPI stopped growth and killed the ERαY537S-4 and ERαD538G-1 cells grown with or without R5020 (Figure 8a-c). Neither growth in a progestin, nor growth in 3D culture, impaired BHPI's impressive ability to block growth and kill ERαY537S-4 and ERαD538G-1 cells.

ICI 182,780 exhibits a reduced ability to induce degradation of ERαY537S and ERαD538G.

ICI induces ERα degradation. Since the ERαY537S-4 and ERαD538G-1 cells were ICI resistant in 3D culture, we examined the effect of ICI and other ligands on levels of ERαY537S and ERαD538G. In the presence of E_2, wild-type ERα exhibited modest down-regulation, which was less evident in the mutants. OHT is a weak agonist and stabilizes ERα. OHT increased levels of ERαY537S but had little effect on the level of ERαD538G. There was a highly significant >2 fold reduction in the ability of ICI to induce degradation of both the double and single replacement ERαY537S and ERαD538G mutants (Figures 10a,b and 11).

a

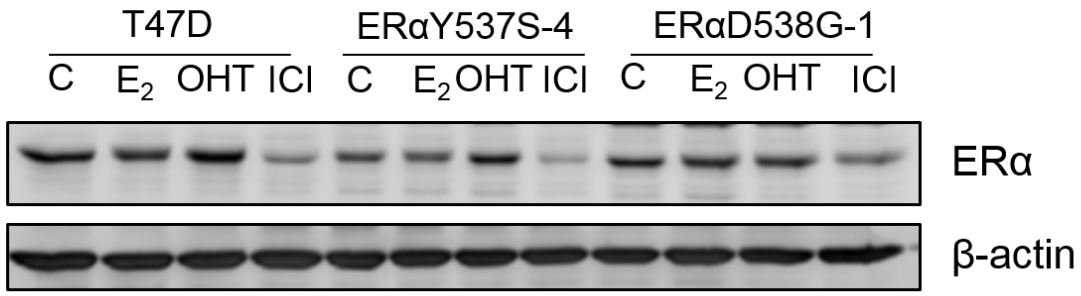

b

Modulation of Wild Type and Mutant ERα by E_2 and Antiestrogens.

Fold ERα	Wild type	ERαY537S	ERαD538G
Ctl	1.00	1.00	1.00
E_2	0.74±0.13	1.04±0.09	0.90±0.04
Z-OHT	1.92±0.16	1.73±0.14	0.99±0.05[b]
ICI	0.21±0.02	0.50±0.06[b]	0.53±0.07[b]

Figure 10. ERαY537S and ERαD538G exhibit altered ligand-dependent degradation. (a) Western blot comparing the effects of E_2, OHT and ICI on levels of ERα in T47D, ERαY537S-4 and ERαD538G-1 cells. Cells were treated with vehicle (C) or 10 nM E_2 (18 hr), or with 1 μM OHT or 1 μM ICI (24 hr). (b) Quantitation of densitometry of ERα levels in ligand-treated T47D, ERαY537S and ERαD538G double replacement cell lines, within each cell line treatments were compared to vehicle control. Data is mean ± SEM (ERαY537S: n=4 cell lines; ERαD538G: n=3

Figure 10 (cont.) cell lines; T47D n=3 experiments); b: p< 0.01 (by Student's T test), for each treatment, comparing mutant to wild-type ERα in T47D cells.

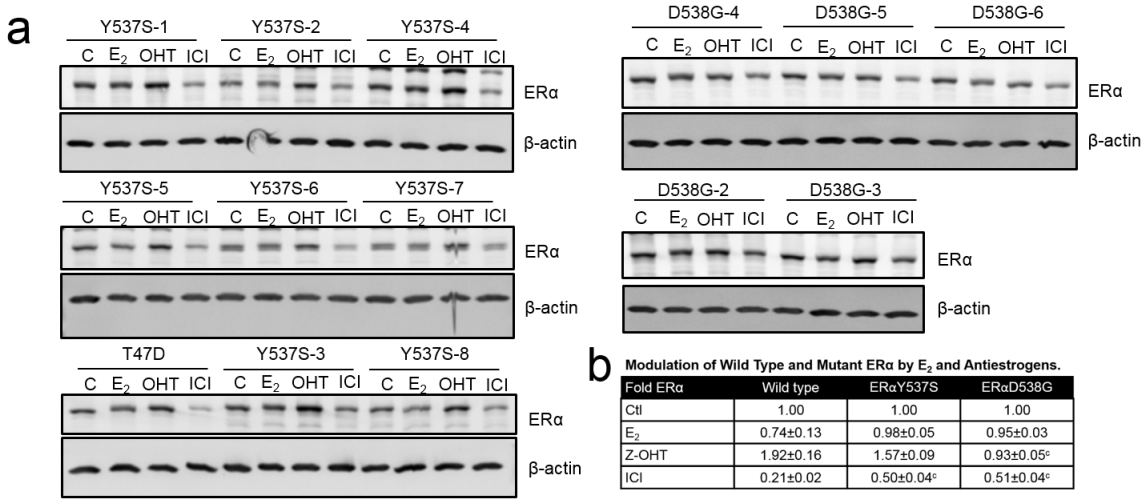

Figure 11. Effects of ligand on ERα degradation in all single and double replacement ERαY537S and ERαD538G cell lines. (a) Western blot analysis (25 μg/lane) and (b) Densitometry of ERα levels in ligand-treated T47D, ERαY537S and ERαD538G cell lines, within each cell line treatments were compared to vehicle. Data in (b) is mean ± SEM (ERαY537S: n=8 cell lines; ERαD538G: n=6 cell lines; T47D: n=3 experiments); b: p< 0.01, c: p< 0.001 (by Student's T test), for each treatment, comparing mutant to wild-type ERα in T47D cells.

Markers of UPR activation are elevated in ERαY537S and ERαD538G cells.

E_2 elicits a weak anticipatory activation of the UPR that is a strong prognostic marker correlated with tamoxifen resistance.[14,79,80] The effect of P_4 on the UPR had not been explored. We therefore investigated the effect of estrogen and progesterone on UPR markers in the tamoxifen-resistant ERαY537S-4 and ERαD538G-1 cells. Activation of the UPR's ATF6α and IRE1α arms induces the strongly oncogenic chaperone BiP/GRP78/HSPA5 by 1.5-3 fold (Figure 12a,c).[81,82] Activation of these UPR arms also induces the anti-apoptotic protein $p58^{IPK}$.[83–85] Pooling data from all 14 mutant cell lines, BiP was significantly elevated in ERαY537S cells and $p58^{IPK}$ was elevated in both ERαY537S and ERαD538G cells (Figure 12b,c). Interestingly, progesterone receptor (PR)

was constitutively elevated to levels higher in ERαY537S and ERαD538G cells than in E_2-treated T47D cells (Figure 12d). P_4 significantly induced levels of BiP and $p58^{IPK}$ in T47D cells and further increased $p58^{IPK}$ in ERαY537S-4 cells, but neither BiP nor $p58^{IPK}$ were significantly further induced in ERαD538G-1 cells (Figure 12e). Thus, progesterone further increases expression of some, but not all, UPR markers.

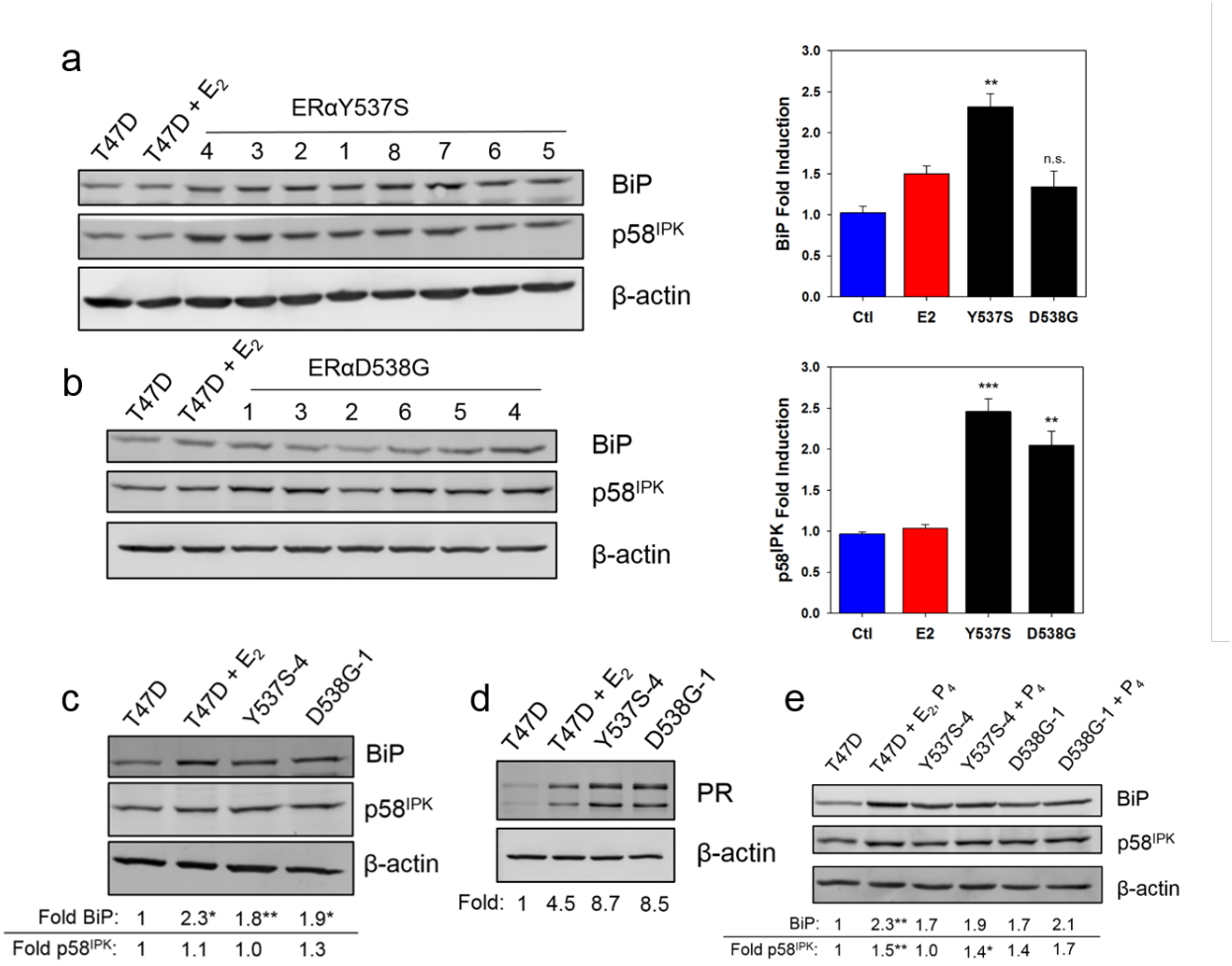

Figure 12. The UPR is activated in ERαY537S-4 and ERαD538G-1 cells and is further activated by progesterone. (a,b) Western blots (left) and quantitation (right) showing BiP and $p58^{IPK}$ induction in all ERαY537S and ERαD538G cell lines. (c) Western blot showing induction of BiP and $p58^{IPK}$ in ERαY537S-4 and ERαD538G-1 cells. (d) Progesterone receptor is highly upregulated in ERαY537S-4 and ERαD538G-1 cells. (e) BiP is strongly induced and $p58^{IPK}$ is induced by P_4 in T47D cells, $p58^{IPK}$ but not BiP is induced by P_4 in ERαY537S-4 cells and neither is significantly induced by P_4 in ERαD538G-1 cells. For (a-e) T47D cells were treated with vehicle or 10 nM E_2 for 24 hr, mutant cell lines were treated with vehicle. In (e) T47D cells were treated

Figure 12 (cont.) with vehicle for 48 hr or with E_2 for 24 hr to induce PR then P_4 for 24 hr; ERαY537S-4 and ERαD538G-1 cells were treated with vehicle or P_4 for 24 hr. Data is mean ± SEM. In (a,b) ERαY537S: n=8 cell lines; ERαD538G: n=6 cell lines; T47D n=3 experiments. In (c,e) quantitation shown below is from the average of three identical blots. *: $p< 0.05$, **: $p< 0.01$, ***: $p< 0.001$ (by Student's T test), for each treatment, comparing each mutant to wild-type vehicle control (a-d) or comparing vehicle treated to P_4 within each cell line (e).

Discussion

While the CRISPR-Cas9 genome editing system has been widely used to inactivate genes,[86–91] gene replacement studies often use a few cell lines exhibiting unusually high HDR frequency.[69–71,92] While our use of 2 guide sequences to increase the frequency of HDR may increase the possibility of off-target events,[93–95] our ability to confirm key observations in 4 ERαY537S and 3 ERαD538G clonal cell lines strongly suggests that the observed properties are due to ERα gene replacement. Because indirect evidence suggests long templates might increase HDR,[96] we used double-stranded templates with 1.2 kb arms, not the short ~50 bp single stranded arms usually used in HDR.[58]

Consistent with the frequency of error-prone NHEJ being much higher than the frequency of HDR,[67–71] all sequenced single replacement clones contained indels in the non-HDR ERα copy. Since ERα in these clones may exist in heterodimers, in which the indel-containing ERα monomer is non-functional, we focused on the double replacement cell lines. Notably, ~30% of cell lines replaced both copies of ERα. This suggests each wild-type ERα copy may undergo multiple NHEJ events before an indel destroys the guide-matched DNA region or a rare HDR event inactivates the PAM sequence.

This work exploited our ability to select for multiple clones expressing ERα mutants that grew out in the absence of E_2. Based on calculations from our large sample size, it seems feasible, but very challenging, to replace genes in typical breast cancer cell lines without a selection. Recent

studies, largely in HEK293 cells, describe methods for increasing the probability of HDR using inhibitors of NHEJ or silencing key molecules involved in NHEJ and optimized HDR templates that target the asymmetric mechanism of Cas9.[69–71]

Our data indicates that the ERαY537S and ERαD538G mutations are sufficient to convert an ERα positive cancer cell, exhibiting E_2-dependent proliferation and growth inhibition by antiestrogens, to one exhibiting E_2-independent proliferation and resistance to high concentrations of OHT and ICI. Importantly, since these experiments were the initial exposure of the ERαY537S and ERαD538G cells to antiestrogens, there was no prior selection for other changes favoring antiestrogen resistance. Consistent with earlier work, E_2-independent proliferation will make tumors expressing these mutations resistant to aromatase inhibitors.

In more biologically relevant anchorage-independent 3D culture, the ERαY537S and ERαD538G cell lines exhibited robust proliferation in the presence of 1 μM z-OHT and 1 μM fulvestrant/faslodex/ICI 182,780 (Figure 8d). Notably, the mutant cell lines continued to proliferate in 5 μM ICI. Since serum ICI in patients is 20-30 nM,[97,98] it is unlikely tumors can concentrate ICI to levels that exceed the 1 and 5 μM in which the mutant cell lines proliferate in 3D culture.

It is widely accepted that ICI is a more nearly pure antagonist than OHT. Since OHT stabilizes and ICI induces degradation of ERα, the ~9 fold lower level of ERα in ICI-treated compared to OHT-treated cells likely makes an important contribution to the increased effectiveness of ICI in T47D cells. However, in the ERαY537S and ERαD538G cell lines, ICI was no more effective in blocking cell growth than OHT, and ICI exhibited a greater than 2 fold reduced ability to induce degradation of the mutant ERαs. Instead of the ~9 fold higher level of ERα in OHT-treated versus ICI-treated T47D cells, the difference in mutant ERα levels was reduced to 2-3 fold. The

diminished ability of ICI to induce degradation of the ERα mutants likely contributes to ICI resistance of ERαY537S and ERαD538G cells. Notably, the ERαY537N mutation is also resistant to ICI-induced degradation.[99] However, in a very recent report, ERαD538G in one patient's circulating tumor cells was not resistant to degradation.[100] This suggests that ICI-induced ERα degradation may also depend on subtle genetic differences in tumors. Of note, using double replacement cell lines may facilitate degradation studies; using current antibodies it is not possible to distinguish between wild type ERα and the mutant ERαs containing these single amino acid changes.

OHT is an antagonist because it induces a different conformational change in ERα than E_2. Very recently, using structural, computational and biophysical approaches Greene and coworkers suggested that the ERαY537S and ERαD538G mutations confer partial antiestrogen resistance because they exhibit reduced affinity for OHT and because they induce a constitutively active conformation that resists deformation by OHT. Moreover, they suggested that ICI, which disorders helix 12 of ERα, might be a therapeutically effective antagonist, blocking activity of ERαY537S and ERαD538G.[43] They also report that ERαY537S is in a conformation that exhibits higher constitutive binding of coactivators than ERαD538G.[43] Our experimental data on differences in proliferation between the ERαY537S and ERαD538G cell lines is consistent with their proposed differences in coactivator interaction. Supporting the view that ERαY537S and ERαD538G are in a constitutively active conformation that resists antiestrogens, proliferation in 3D culture is constitutive and largely resistant to saturating OHT and ICI.

In breast cancer cells expressing wild type ERα and PR, progesterone increases stemness and markers associated with therapy resistance.[72] Moreover, progesterone can be mitogenic and mediate cell survival in 3D cultures.[72] However, recent xenograft and explant studies show that

when estrogen is present, progestins enhance sensitivity of breast cancers expressing wild type ERα to tamoxifen.[74] Consistent with an earlier study,[101] PR was constitutively expressed to extremely high levels in the ERαY537S and ERαD538G cells, suggesting it might play an important role. We report that a progestin decreases sensitivity of ERαY537S and ERαD538G cells to growth inhibition by OHT and ICI in both 2D and 3D culture. In 3D cultures treated with a progestin, 1 μM OHT and ICI have lost the ability to inhibit proliferation of ERαY537S and ERαD538G cells. Since progestin had little ability to reverse OHT and ICI inhibition of T47D cell growth, the progestin effect is likely related to the ERαY537S and ERαD538G mutations. Consistent with the possibility that serum progestin might influence antiestrogen resistance in women whose breast cancers express the ERαY537S and ERαD538G mutations, progesterone levels in post-menopausal women are 0.6-3 nM.[102–104] Moreover, breast cancer cells expressing both ERα and PR, or overexpressing PR alone, may be sensitive to very low concentrations of hormone.[72,73] Since the ERαY537S and ERαD538G cells constitutively express very high levels of PR, the low serum concentrations of progestins in postmenopausal women together with high PR could well have functional effects on antiestrogen resistance in metastatic breast cancers expressing ERα mutations.

Weak activation of the UPR is protective in cancer and is associated with a poor prognosis, while extensive and sustained UPR activation by BHPI is toxic.[29,36,79,80] Since we cannot currently analyze protein levels in cells from 3D cultures in soft agar, the UPR studies were carried out in standard 2D cell culture. The ERαY537S cells exhibited constitutive activation of the IRE1α arm of the UPR, as indicated by estrogen-independent induction of the oncogenic chaperone BiP. In contrast, the ERαD538G cells exhibited a much smaller induction of BiP. This is consistent with the ERαD538G mutant showing a lower level of constitutive growth and antiestrogen resistance

in cell proliferation. Since our 2D cell culture data shows that ERαY537S cells exhibit significant resistance to OHT and ICI and the ERαD538G cells exhibited very little resistance (Figure 8c), this data is consistent with a link between constitutive UPR activation and antiestrogen resistance. However, while constitutive UPR activation likely contributes to the antiestrogen resistant phenotype seen in the ERαY537S and ERαD538G cell lines, the extent to which it does is unclear, and effects are likely complex.

In 2D culture R5020 increased proliferation of the ERαY537S and ERαD538G cells in OHT and ICI; in 3D culture, R5020 abolished growth inhibition by OHT and ICI. This effect of progestin-PR may not only be mediated through further activation of the UPR but also through modulation of ERα action and PR's own transcriptomic program.[74] Although further study is needed, progestins seem likely to enhance antiestrogen effectiveness in cancer cells expressing the ERαY537S and ERαD538G mutations.

Although the mutations exhibit an altered ERα conformation,[5] and are close to the proposed BHPI binding site,[29] BHPI was as effective in blocking proliferation of all 14 of the ERαY537S and ERαD538G cell lines as it was in T47D cells. Moreover, in 3D culture where the ERαY537S-4 and ERαD538G-1 cells exhibited robust proliferation in 1 μM OHT and ICI, 100 nM BHPI completely blocked proliferation and killed the cells.

We used the CRISPR-Cas9 genome editing system to generate precise replacements of both copies of a steroid receptor gene. Breast cancer cell lines expressing these ERα mutations associated with metastatic breast cancer are highly resistant to endocrine therapy. Taken together, our data and the recent structural and biophysical studies suggest that a constitutively active ERα conformation, altered ICI-induced degradation of ERα, progestin and UPR activation may all

contribute to the antiestrogen resistant phenotype. Notably, the preclinical drug candidate BHPI retains its effectiveness against these resistant breast cancer cells.

CHAPTER 4: STRONG AND SUSTAINED ACTIVATION OF THE ANTICIPATORY UNFOLDED PROTEIN RESPONSE INDUCES NECROTIC CELL DEATH

This work contains previously published material.[3]

Abstract

The endoplasmic reticulum stress sensor, the unfolded protein response (UPR), regulates intracellular protein homeostasis. While transient activation of the reactive UPR by unfolded protein is protective, prolonged and sustained activation of the reactive UPR triggers CHOP-mediated apoptosis. In the recently characterized, evolutionarily conserved anticipatory UPR, mitogenic hormones and other effectors pre-activate the UPR; how strong and sustained activation of the anticipatory UPR induces cell death was unknown. To characterize this cell death pathway, we used BHPI, a small molecule that activates the anticipatory UPR through estrogen receptor α (ERα) and induces death of ERα$^+$ cancer cells. We show that sustained activation of the anticipatory UPR by BHPI kills cells by inducing depletion of intracellular ATP, resulting in classical necrosis phenotypes, including plasma membrane disruption and leakage of intracellular contents. Unlike reactive UPR activation, BHPI-induced hyperactivation of the anticipatory UPR does not induce apoptosis or sustained autophagy. BHPI does not induce CHOP protein or PARP cleavage, and two pan-caspase inhibitors or Bcl2 overexpression have no effect on BHPI-induced cell death. Moreover, BHPI does not increase expression of autophagy markers, or work through recently identified programmed-necrosis pathways, such as necroptosis. Opening of endoplasmic reticulum IP_3R calcium channels stimulates cell swelling, cPLA2 activation, and arachidonic acid

[3] Livezey, M. et al. Cell Death & Differentiation, 2018. Data in Figures 13(c-e), 14(a,e), 16(a,b), 17(a,b), 18(a,c,d), 19d, 23(b,d,e), and 24b was obtained in whole or in part by Ms. Rui Huang working under my supervision. Reference 153.

release. Notably, cPLA2 activation requires ATP depletion. Importantly, blocking rapid cell swelling or production of arachidonic acid does not prevent necrotic cell death. Rapid cell death is upstream of PERK activation and protein synthesis inhibition, and results from strong and sustained activation of early steps in the anticipatory UPR. Supporting a central role for ATP depletion, reversing ATP depletion blocks rapid cell death, and the onset of necrotic cell death is correlated with ATP depletion. Necrotic cell death initiated by strong and sustained activation of the anticipatory UPR is a newly discovered role of the UPR.

Introduction

The unfolded protein response (UPR) is an endoplasmic reticulum (EnR) stress-response pathway that maintains protein folding homeostasis and quality control. Three UPR arms, PERK, IRE1α, and ATF6α, act together to decrease the flux of new protein into the EnR, while upregulating molecular chaperones that help fold protein.[2,27] Due to its protective effects when weakly activated, the UPR is implicated in the development of numerous cancers.[3,28,80,81] In this reactive mode of UPR activation, accumulation of unfolded or misfolded protein triggers UPR activation. A different pathway of UPR activation, originally identified in immune cells and recently shown to be activated by the mitogenic hormones, estrogen, EGF, and VEGF, pre-activates the UPR, anticipating future requirements for increased protein folding capacity.[12–14] Demonstrating clinical relevance, data from ~1000 estrogen receptor α positive ($ER\alpha^{+}$) breast cancers shows that activating a UPR gene signature is a powerful prognostic marker, tightly correlated with subsequent resistance to tamoxifen, reduced time to recurrence, and reduced survival.[14]

Strong and sustained activation of the reactive UPR induces caspase-dependent apoptosis. Activation of PERK inhibits translation of most mRNAs, increasing translation of ATF4 (activating transcription factor 4). ATF4 induces the transcription factor CHOP (C/EBP homologous protein) and subsequently GADD34 (growth arrest and DNA-damage-inducible protein 34).[1,2,50–52] When these factors reach a critical threshold and the UPR-activating stress cannot be resolved, apoptosis is triggered.[1,2,50–52]

The consequences of strong and sustained activation of the anticipatory UPR were largely unknown. We described a small molecule, BHPI, that is a potent preclinical anticancer drug.[15,29,36,80] Unlike inhibitors targeting the reactive UPR, BHPI works by inducing hyperactivation of the anticipatory UPR.[29,35,52,105,106] BHPI acts through ERα to induce rapid activation of phospholipase C γ (PLCγ), which cleaves PIP_2 to diacylglycerol (DAG) and inositol triphosphate (IP_3). IP_3 then binds to and opens IP_3 receptors (IP_3Rs) in the EnR membrane, allowing efflux of calcium stored in the lumen of the EnR into the cell body. This robust and sustained calcium efflux leads to strong and sustained activation of all three arms of the UPR.[29] Through this pathway, BHPI blocks proliferation of, and often kills, $ER\alpha^+$ breast, endometrial, and ovarian cancer cells.[15,29,36]

Here we describe how sustained activation of the anticipatory UPR by BHPI kills cancer cells. In contrast to classical UPR activators that kill cells through caspase-dependent apoptosis,[50–52] BHPI hyperactivates the anticipatory UPR; this causes ATP depletion leading to cell death by a necrosis-like mechanism. Notably, in parallel with necrosis, hyperactivation of the anticipatory UPR activates production of arachidonic acid and causes cell swelling.

Results

BHPI Kills ERα$^+$ Breast and Endometrial Cancer Cells

BHPI targets ERα$^+$ cancer cells by inducing activation of the anticipatory UPR.[29,36] In cell culture, conventional endocrine therapies for breast cancer, tamoxifen and fulvestrant/ICI 182,780 (ICI), inhibit estrogen-ERα-dependent proliferation and usually do not kill cancer cells. To explore whether BHPI induces cell death, we performed proliferation assays using tamoxifen-resistant TamR cells,[107] T47D cells, and cell lines expressing ERα mutations common in metastatic breast cancer: T47D-ERαY537S (TYS) and T47D-ERαD538G (TDG).[15] BHPI not only blocked growth, but also reduced cell number below that initially plated, indicating cell death (Figure 13a,b). To better quantify cell death, we used an automated assay for cell viability, trypan blue exclusion. Consistent with action through ERα, BHPI caused cell death in as little as 24 hours in ERα$^+$ cell lines, but not in ERα$^-$ cell lines (Figure 13c-e).

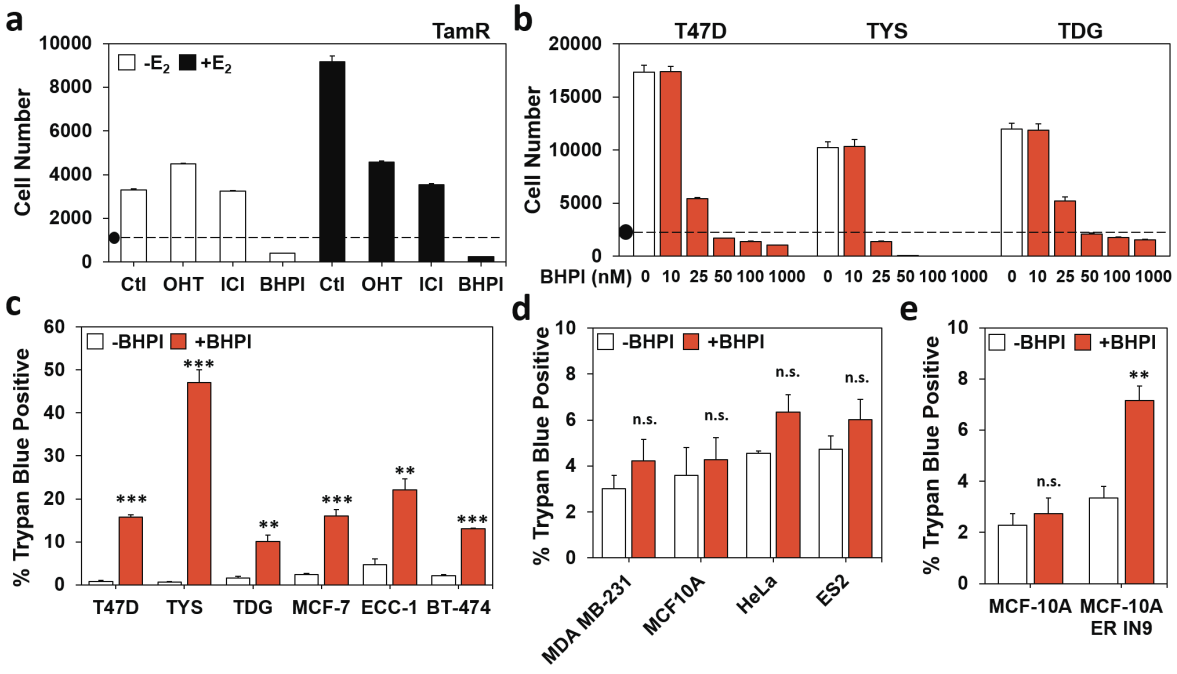

Figure 13. BHPI kills ERα+ breast and endometrial cancer cells. (a) TamR cell proliferation after 4 days in 8% charcoal:dextran-treated calf (CD-calf) serum with the indicated treatments:

Figure 13 (cont.) E_2 100 pM; z-4-hydroxytamoxifen (OHT, the active form of tamoxifen) 1 μM; ICI/fulvestrant 1 μM; BHPI 100 nM. (•) Indicates starting cell number (day 0). (b) Dose-response study of the effect of increasing concentrations of BHPI on proliferation of T47D, TYS, and TDG cells after 4 days. (a, b) Alamar-blue assays; (n=8 biological replicate experiments). (c) Automated trypan blue exclusion assays of ERα-positive cells after 24 hr treatment with 1 μM BHPI. (d) Trypan blue exclusion assays of ERα-negative cells after 24 hr treatment with 1 μM BHPI. (e) Trypan blue exclusion assays of isogenic MCF10A and $MCF10A_{ER\ IN9}$ cells after 24-hour treatment with 1 μM BHPI. (c-e) Data is mean ± s.e.m (n=3 biological replicate experiments). For (c-e) **p<0.01, ***p<0.001, n.s. = not significant by Student's T-test.

Unlike Classical UPR Activators, BHPI Does Not Induce Caspase-dependent Apoptosis

Consistent with activation of caspase-dependent apoptosis, the pan-caspase inhibitor Q-VD-OPH blocks cell death induced by reactive UPR activators, thapsigargin (THG) and bortezomib (BORT) (Figure 14a).[50–52,108] In contrast, BHPI-induced cell death through hyperactivation of the anticipatory UPR is not blocked by the pan-caspase inhibitors Q-VD-OPH or Z-VAD-FMK at 1 (TYS) or 24 hours (T47D and TDG) (Figures 14b and 15a), or by transient overexpression of Bcl2 in TYS cells (Figure 14c). Furthermore, Z-VAD-FMK had no effect on BHPI's ability to block growth of T47D, TYS, or TDG cells over 4 days (Figure 15b). Consistent with earlier reports of impaired caspase-dependent apoptosis in MCF-7 and T47D cells,[109–111] we saw only minor PARP (poly ADP-ribose polymerase) cleavage upon treatment of T47D, BT-474, or ECC-1 cells with the apoptosis-inducer and general protein kinase inhibitor staurosporine (STS), as well as no visible PARP cleavage with BHPI up to 48 hours (Figure 14d). Characteristic of apoptotic cell death, STS-treatment of TYS cells caused a distinct increase in Annexin V-FITC staining, followed by propidium iodide (PI) uptake into cells, as determined by flow cytometry. In contrast, BHPI-treated cells exhibited a markedly different staining pattern (Figure 15c,d).

Reactive UPR activators upregulate the mediator of the UPR-induced apoptotic cascade, CHOP.[112–114] We show BHPI upregulates CHOP mRNA, but due to rapid, sustained, near-

quantitative inhibition of protein synthesis through PERK activation,[29] CHOP protein is never made (Figure 14e).

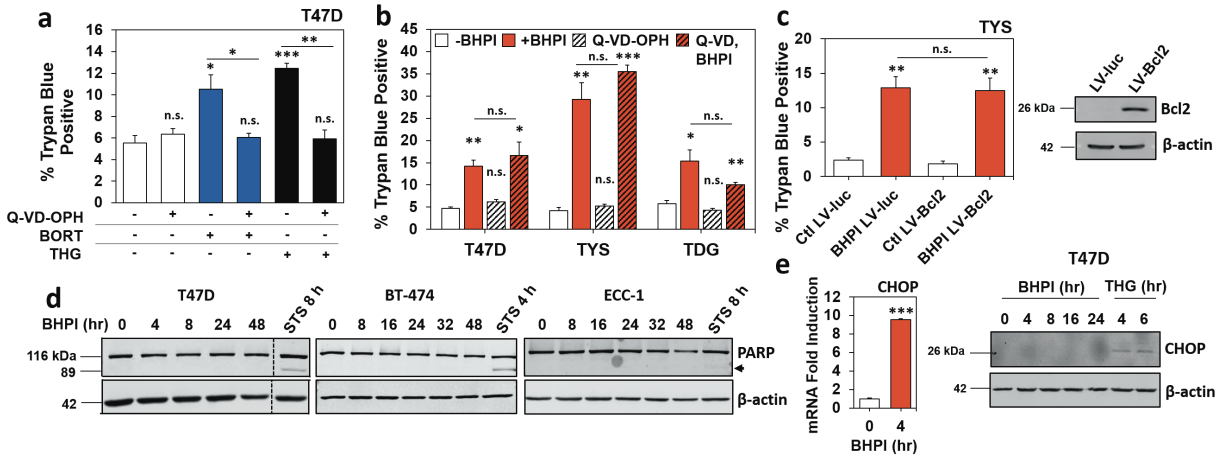

Figure 14. BHPI does not induce caspase-dependent apoptosis. (a) Trypan blue exclusion assay of T47D cells after 24 hr treatment with or without 20 μM Q-VD-OPH, 100 nM bortezomib (BORT), or 10 μM thapsigargin (THG). (b) Trypan blue exclusion assay of T47D and TDG cells after 24 hr, and TYS cells after 1 hr treatment with: 1 μM BHPI with or without 20 μM Q-VD-OPH. (c) Trypan blue exclusion assay and western blot analysis of TYS cells infected with lentivirus expressing luciferase (LV-luc) or Bcl2 (LV-Bcl2) after 1 hr treatment with 1 μM BHPI. (a,b,c) Data is mean ± s.e.m (n=3 biological replicate experiments), *p<0.05, **p<0.01, ***p<0.001, n.s.= not significant by Student's T-test. (d) Western blot analysis of cleaved PARP (arrow) in T47D and BT-474 breast cancer cells, and ECC-1 endometrial cancer cells after treatment with 1 μM BHPI or 5 μM staurosporine (STS) for the indicated times. (e) mRNA and western blot analysis of CHOP induction in T47D cells treated with 1 μM BHPI or 300 nM thapsigargin (THG) for the indicated times.

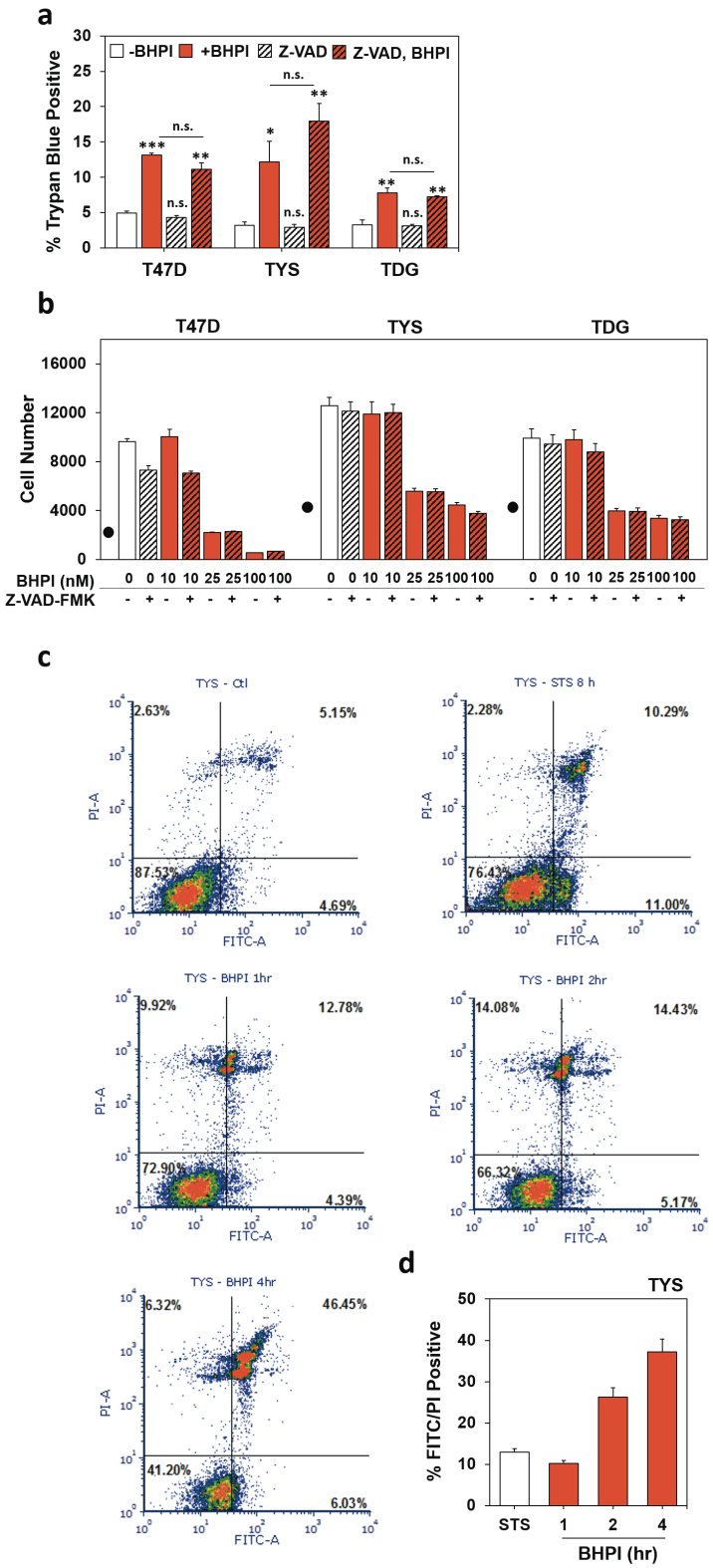

Figure 15. BHPI does not kill cells through apoptosis. (a) Trypan blue exclusion assay of T47D and TDG cells after 24 hr, and TYS cells after 1 hr treatment with: 1 µM BHPI with or without 20 µM Z-VAD-FMK. (b) T47D, TYS, and TDG cell proliferation after 4 days in complete

Figure 15 (cont.) growth medium with the indicated concentration of BHPI with or without 20 μM Z-VAD-FMK. Alamar-blue assay. (•) indicates initial number of cells plated. (c) Representative flow cytometry histograms of annexin V-FITC (FITC) and propidium iodide (PI) staining of TYS cells after treatment with 5 μM staurosporine (STS) for 8 hours or 1 μM BHPI for the indicated times. (d) Percent annexin V-FITC (FITC) and/or propidium iodide (PI) positive TYS cells relative to vehicle control. Data is mean ± s.e.m (a,c) (n=3 biological replicate experiments); (b) (n=8 biological replicate experiments) *$p<0.05$, **$p<0.01$, ***$p<0.001$, n.s. = not significant by Student's T-test.

BHPI Does Not Upregulate Autophagy

The contribution of autophagy to cancer is complex. Mild induction of autophagy is protective, while extended activation is toxic.[115–117] Using the inhibitor of lysosomal acidification, chloroquine (CQ), we blocked turnover of proteins in the autophagosome and monitored the production of the autophagy marker LC3-II.[115,116] Surprisingly, BHPI down-regulated LC3-II in T47D, TYS, TDG, and ECC-1 cells (Figure 16a). A second autophagy marker, Beclin-1,[115,118] was unchanged or down-regulated in T47D, TYS, and TDG cells (Figure 16b). Lastly, we probed the central regulator of cell metabolism, mTOR (mammalian target of rapamycin). Nutritional deficiency inhibits mTOR and activates autophagy.[115,119,120] To monitor mTOR activation, we looked at a downstream readout of active mTOR, phosphorylated p70S6K. Similar to 24-hour serum starvation, BHPI caused a transient decrease in p70S6K phosphorylation at 8 hours, but p70S6K phosphorylation recovered and was stable from 16-48 hours (Figure 16c). This indicates extended BHPI treatment leads to mTOR activation and inhibition of autophagy.

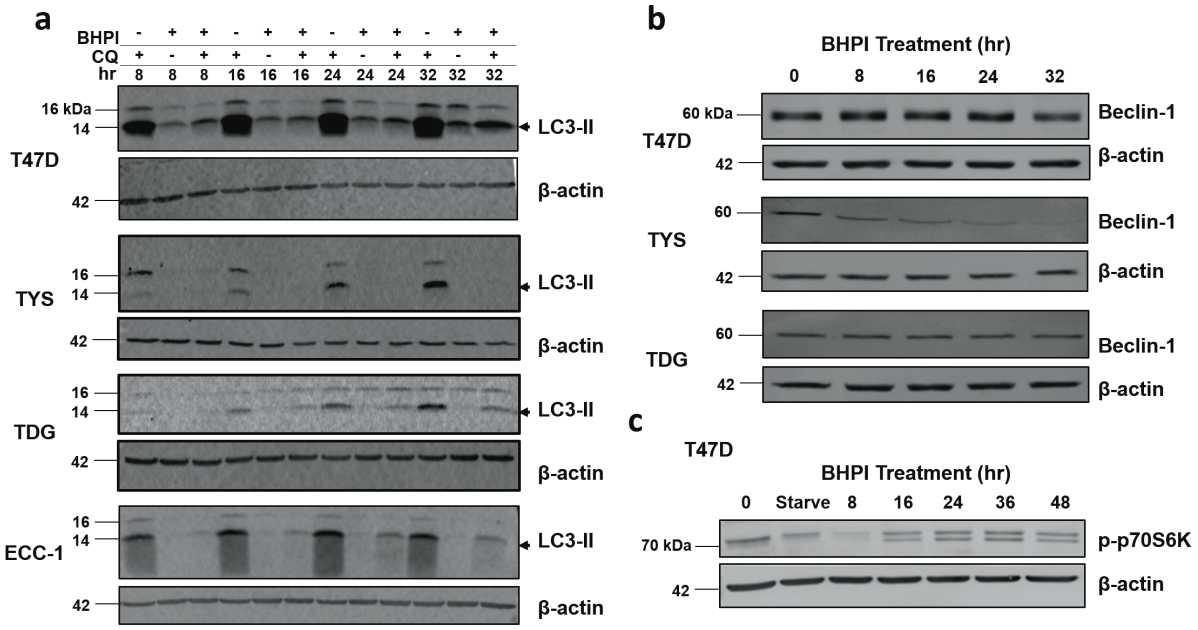

Figure 16. Autophagy is not upregulated by BHPI. (a) Western blot analysis of LC3-II production (arrow) in T47D, TYS, TDG, and ECC-1 cells after treatment with 1 μM BHPI, 30 μM Chloroquine (CQ), or BHPI + CQ for the indicated times. (b) Western blot analysis of Beclin-1 levels in T47D, TYS, and TDG cells after treatment with 1 μM BHPI for the indicated times. (c) Western blot analysis of phosphorylation of p70S6K in T47D cells after treatment with 1 μM BHPI for the indicated times, or after serum starvation (Starve) for 24 hrs.

BHPI Induces Rapid Swelling of Cancer Cells

While there was no evidence for BHPI-induced programmed cell death, we noticed that hours after BHPI treatment, cells appeared swollen. Swelling is associated with diverse lethal pathologies, including edema, hypertrophy, and necrosis.[121] BHPI, but not the inactive structurally-related compound 8, caused concentration-dependent cell swelling (Figure 17a).[29] Cell swelling is ERα-dependent; $ERα^+$ cell lines exhibited significant swelling within 1 hour, while $ERα^-$ cell lines did not (Figure 18a,b). Moreover, siRNA knockdown of ERα (ESR1) significantly attenuated swelling. Since knockdown was incomplete and BHPI is an extremely potent activator of the anticipatory UPR, some residual swelling was observed (Figure 17b). Interestingly, rapid swelling was closely followed by an increase in death in TYS and MCF-7 cells (Figure 18c).

The mitogenic hormones estrogen (E_2), EGF, and progesterone (P_4) weakly activate the anticipatory UPR.[13–15] Demonstrating the unique ability of BHPI to cause cell swelling, weak activation of the anticipatory UPR by E_2, EGF, and P_4 did not induce swelling (Figure 17c). Additionally, reactive UPR activators bortezomib (BORT) and tunicamycin (TUN) did not cause swelling (Figure 17d). Although the reactive UPR activator THG and BHPI produce similar increases in cytosolic calcium,[29] THG did not cause swelling (Figure 17e). Moreover, the endocrine therapies z-4-hydroxytamoxifen (OHT) and ICI/fulvestrant or the chemotherapeutic doxorubicin (DOX) did not cause cell swelling, and paclitaxel (PAC) caused minimal swelling (Figure 17d).

Since BHPI was unique in its ability to cause rapid swelling, we asked whether this was specific to hyperactivation of the anticipatory UPR. We showed that 2-APB completely blocks calcium release from EnR IP_3R channels following BHPI treatment and after weak activation of the anticipatory UPR.[14,29,122] 2-APB blocked BHPI-induced swelling (Figure 18d). Supporting BHPI acting through anticipatory UPR hyperactivation, BHPI induced swelling in T47D cells maintained in calcium-free medium (Figure 18d). Moreover, the calcium chelator, BAPTA-AM, completely blocked swelling (Figure 18d). We hypothesized that BHPI might be eliciting cell swelling by modulating ion channels. However, inhibitors targeting individual ion channels/pumps did not block swelling (Figure 18e). Since BHPI was not able to swell cells in salt-free, isosmotic medium, extracellular ions are necessary for BHPI-induced swelling (Figure 18f). Taken together, this suggests that BHPI hyperactivation of the anticipatory UPR triggers cell swelling, and that non-specific increases in cytosolic calcium, or activation of the reactive UPR, do not trigger cell swelling.

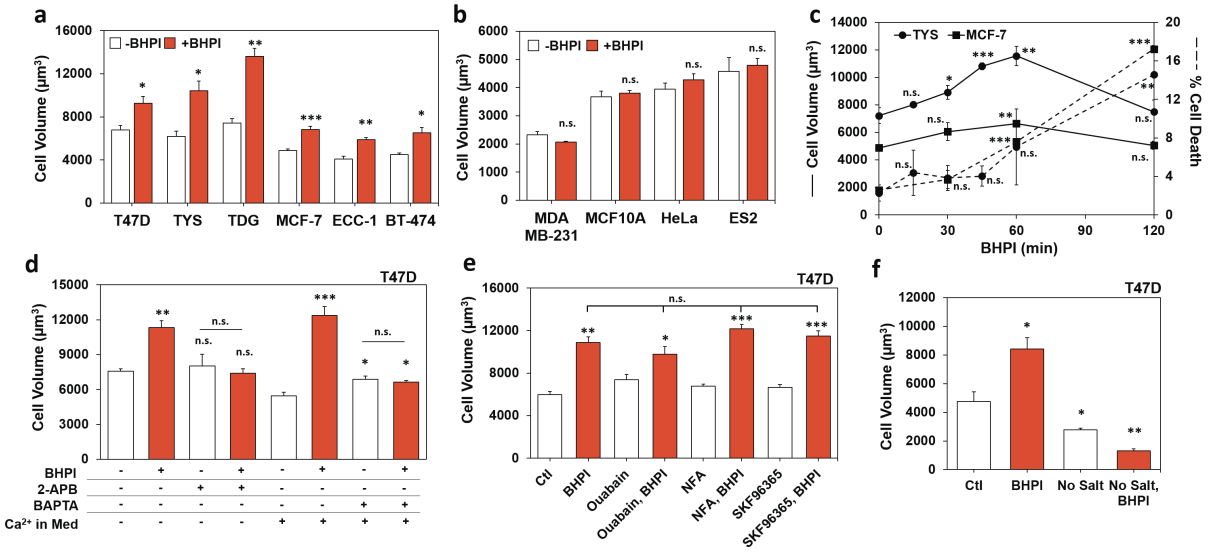

Figure 17. BHPI-ERα-induced cell swelling is linked to early steps in the anticipatory UPR. (a) Cell volume in ERα-positive cells treated with 1 µM BHPI for 1 hr (T47D, TYS, TDG, MCF-7 and BT-474), or 30 min (ECC-1). (b) Cell volume in ERα-negative MDA MB-231, MCF10A, HeLa, and ES2 cells treated with 1 µM BHPI for 1 hr. (c) Time course of the effect of BHPI on cell volume and cell death in TYS and MCF-7 cells. Cell volume (solid lines) and cell death (dashed lines) were assayed by trypan blue exclusion in cells treated with 50 nM BHPI (TYS), or 100 nM BHPI (MCF-7). (d) Blocking the increase in intracellular calcium with 2-APB, or with the calcium chelator, BAPTA-AM (BAPTA), prevents the BHPI-induced increase in cell volume. Cell volume in T47D cells treated for 1 hr with vehicle, 50 nM BHPI, 100 µM 2-APB, or BHPI + 2-APB in calcium-free isosmotic medium, or vehicle, 20 µM BAPTA-AM, or BHPI + BAPTA-AM. (e,f) Cell volume of T47D cells after 1 hr treatment as indicated. (e) BHPI 50 nM; ouabain 2 µM (Na^+/K^+ ATPase inhibitor); niflumic acid (NFA) 100 µM (nonspecific anion channel inhibitor); SKF96365 10 µM (TRP channel inhibitor). (f) BHPI 50 nM; isosmotic salt-free sucrose buffer (No Salt). Data is mean ± s.e.m (n=3 biological replicate experiments) *p<0.05, **p<0.01, ***p<0.001, n.s. = not significant by Student's T-test.

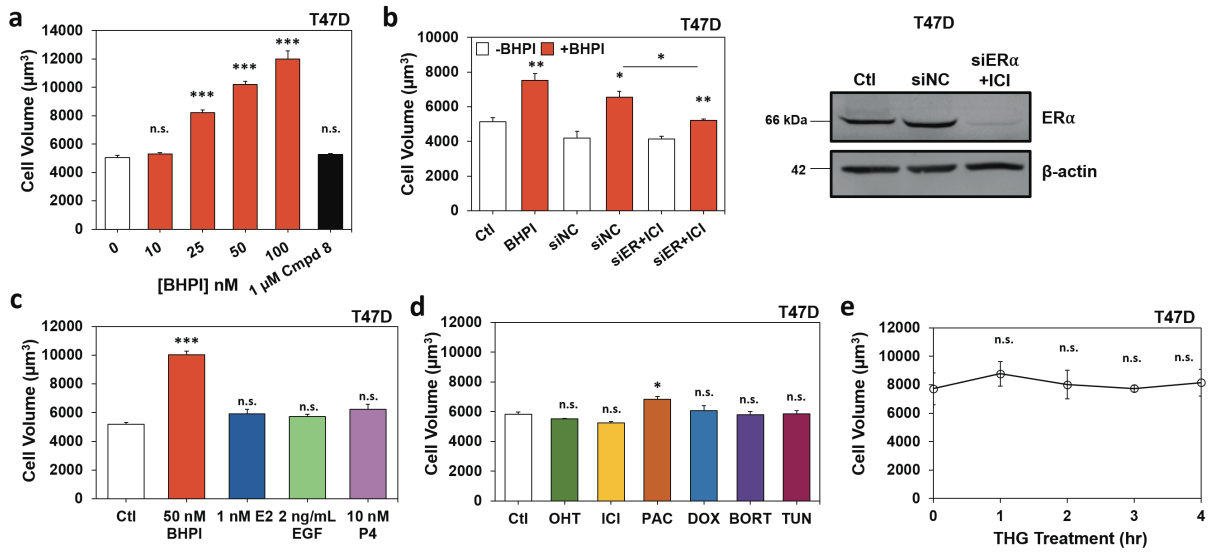

Figure 18. BHPI-induced cell swelling is ERα-dependent and unique to anticipatory hyperactivation of the UPR. (a) Dose-response study of cell volume in T47D cells treated for 1 hr with the indicated concentrations of BHPI, or the inactive structurally-related compound 8 (Cmpd 8). (b) Effect of reducing ERα levels on cell volume and western blot analysis of ERα in T47D cells. Cells were plated and treated with non-coding (siNC) or ERα (siERα) siRNA for 16 hr. 24 hr later, cells were treated with ICI for 24 hr to further reduce the levels of ERα before measurement of cell volume in T47D cells treated with vehicle or 1 μM BHPI for 1 hr, with the indicated pre-treatment: non-coding siRNA 100 nM; ERα siRNA 100 nM + ICI 1 μM. (c-e) Cell volume of T47D cells after the indicated treatments for 1 hr, or as noted. z-4-hydroxytamoxifen (OHT) 1 μM; ICI 1 μM; paclitaxel (PAC) 1 μM; doxorubicin (DOX) 1 μM; bortezomib (BORT) 100 nM; tunicamycin (TUN) 10 μg/mL; thapsigargin (THG) 1 μM. Data is mean ± s.e.m (n=3 biological replicate experiments) *p<0.05, **p<0.01, ***p<0.001, n.s. = not significant by Student's T-test.

BHPI Activation of cPLA2 Leads to Arachidonic Acid Release

Calcium signaling and membrane stretching activate cytosolic phospholipases A2 (cPLA2s), resulting in cleavage of membrane phospholipids to form arachidonic acid (AA).[123–125] AA and its metabolites can further alter cell volume by modulating the activity of ion channels.[126] Additionally, AA induces death in glial cells.[127] BHPI elicited time-dependent AA release in T47D cells and AA release correlated with cell swelling (Figure 19a). Furthermore, within 1 hour, BHPI induced concentration-dependent release of AA from several cell lines (Figure 19b). Neither

control compound 8 (Figure 20a) nor THG (Figure 19c) caused release of AA, but THG was able to block BHPI-induced AA release (Figure 19c). Importantly, THG did not block swelling in T47D or TYS cells, indicating membrane stretching is not sufficient to activate cPLA2 (Figure 20b). Consistent with cPLA2 as the source of AA, the cPLA2 inhibitor quinacrine (Quin) blocked release of AA from T47D cells (Figure 19c). Suggesting AA contributes minimally to cell swelling, adding AA to culture medium increased cell size modestly (Figure 20c). Additionally, while Quin blocked cell swelling, the block was only partially reversed by adding back AA (Figure 19d).

Demonstrating that neither AA release nor cell swelling are directly related to rapid cell death, while Quin blocked both AA release and swelling, it did not block death in TYS cells, which die rapidly following BHPI treatment (Figure 19e). Although AA is the precursor for pro-inflammatory prostaglandins, BHPI treatment for 24 hours only elicited a minimal increase in prostaglandin (Figure 19f).[128,129]

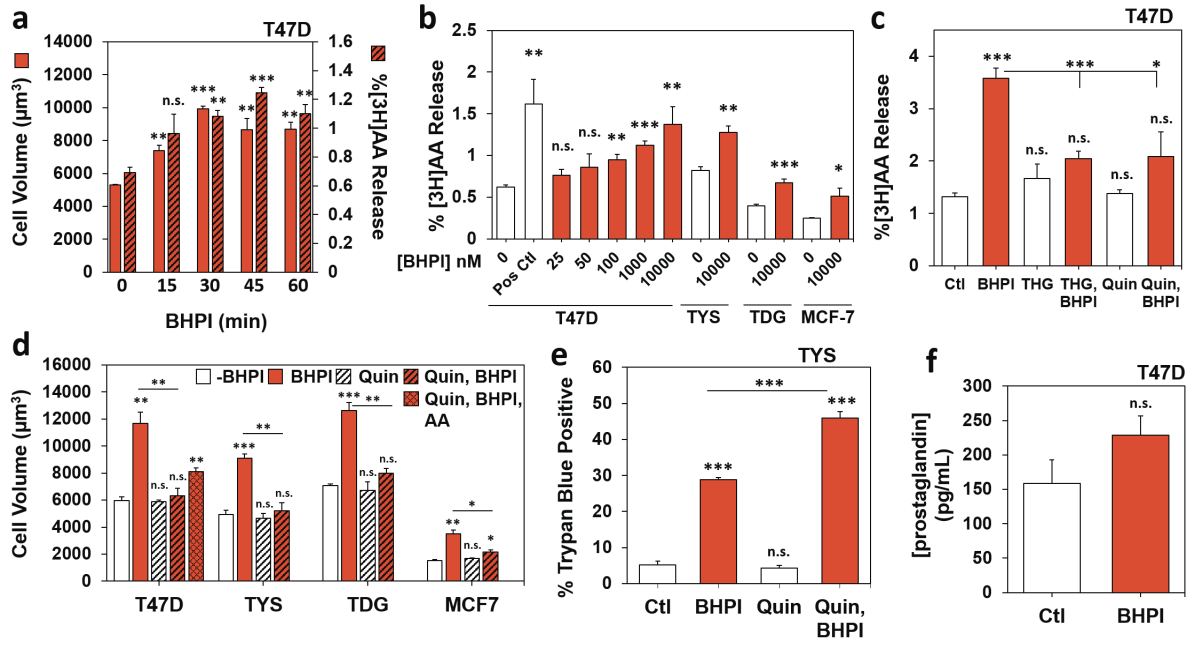

Figure 19. BHPI activation of cPLA2 causes release of arachidonic acid (AA). (a) Time course showing a correlation between increased AA release and increased cell volume in BHPI-treated T47D cells. Time course of changes in cell volume (solid bars) and ^{3}H-arachidonic acid release ([^{3}H]AA, hatched bars) after treatment of T47D cells with vehicle or with 10 μM BHPI. Data is mean ± s.e.m (solid bars, n=3 biological replicate experiments; hatched bars, n=4 biological replicate experiments). (b) Concentration-dependent release of [^{3}H]AA from T47D, TYS, TDG, and MCF-7 cell membranes after treatment for 45 min with vehicle or the indicated concentration of BHPI. Positive control (Pos Ctl) is 150 mOsm buffer with 1 μM THG. (c) THG and the cPLA2 inhibitor quinacrine (Quin) block the BHPI-mediated increase in AA. Release of [^{3}H]AA from T47D cell membranes after treatment for 45 min with vehicle, 1 μM thapsigargin (THG), 1 μM BHPI, BHPI + THG, 300 μM Quin, or BHPI + Quin. (d) Effect of Quin and AA on BHPI-induced changes in cell volume. Volume of T47D, TYS, TDG, and MCF-7 cells after treatment for 1 hr with vehicle, 50 nM BHPI, 300 μM Quin, 250 μM AA, BHPI + Quin, or BHPI + Quin + AA. (e) Quin does not block BHPI-induced cell death. Trypan blue exclusion assay for cell death in TYS cells treated for 1 hr with vehicle, 1 μM BHPI, 300 μM Quin, or BHPI + Quin. (f) ELISA determination of prostaglandin production from T47D cells after treatment for 24 hr with 10 μM BHPI. Data is mean ± s.e.m (b,c,f) (n=4 biological replicate experiments), (d-e) (n=3 biological replicate experiments). For (a-f) *p<0.05, **p<0.01, ***p<0.001, n.s. = not significant by Student's T-test.

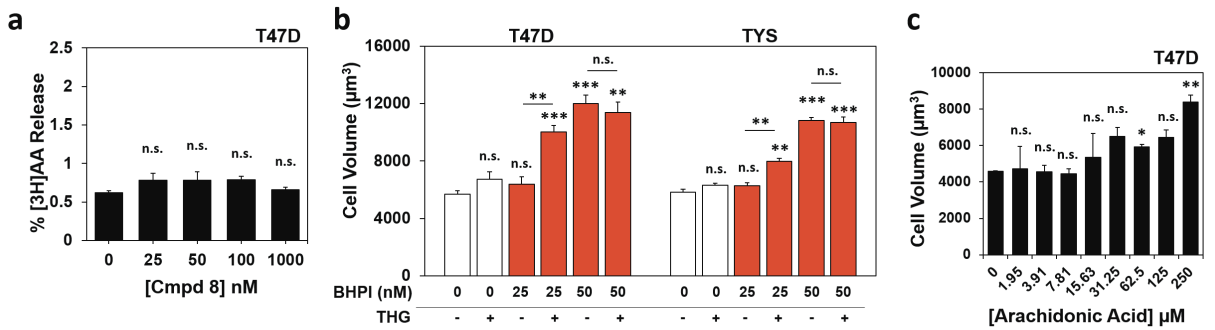

Figure 20. AA only modestly modulates cell volume. (a) Release of [^{3}H]AA after 45 min treatment with inactive BHPI relative, compound 8. (b) THG does not block the BHPI-mediated increase in cell volume. Cell volume in T47D and TYS cells treated for 1 hr with vehicle, 1 µM THG, 25 or 50 nM BHPI and 25 or 50 nM BHPI + THG. (c) Dose-response study of the effect of AA on cell volume. T47D cells were treated for 1 hr with the indicated concentrations of AA. Data is mean ± s.e.m. For (a) (n=4 biological replicate experiments), (b,c) (n=3 biological replicate experiments) *p<0.05, **p<0.01, ***p<0.001, n.s. = not significant by Student's T-test.

BHPI Induces Necrotic Cell Death

While neither swelling nor AA production is responsible for rapid cell death, they are associated with inflammatory forms of cell death, such as necrosis. Necrotic cell death has fewer well-defined markers than apoptosis or autophagy; necrosis often involves disruption of calcium homeostasis, cell swelling, ATP depletion and, ultimately, loss of plasma membrane integrity.[38,56,130,131] We observed loss of membrane integrity in T47D, TYS, and TDG cells by monitoring leakage of cellular HMGB1 (high mobility group box 1) (Figure 21a) and LDH (lactate dehydrogenase) into the medium (Figure 22a). Necrosis is best assessed by morphological changes visualized by transmission electron microscopy (TEM). TEM images of T47D, TYS, and TDG cells treated with BHPI for 24 or 48 hours revealed morphological changes characteristic of necrosis, including lysosomal and mitochondrial swelling, translucent cytoplasm, and ultimately, plasma membrane disintegration (Figures 21b and 22b).[56,131,132] Cells treated with BHPI were similar to cells treated with a necrosis-inducing concentration of H_2O_2 for 24 hours (Figure 22b).[133]

There is increasing interest in programmed necrosis, or necroptosis. Initiation of necroptosis by diverse stimuli requires receptor-interacting proteins 1 or 3 (RIP1, RIP3).[134,135] To test the involvement of RIP1 and RIP3, we used the inhibitors 7-Cl-O-Nec-1 (Nec-1) and GSK872, respectively. Nec-1 and GSK872 did not reduce killing by BHPI at 1 (TYS) or 24 hours (T47D and TDG), failed to restore proliferation over 4 days, and instead, increased cell death (Figure 22c,d). Independent of necroptosis, these compounds are known to inhibit cell proliferation and induce apoptosis.[135,136]

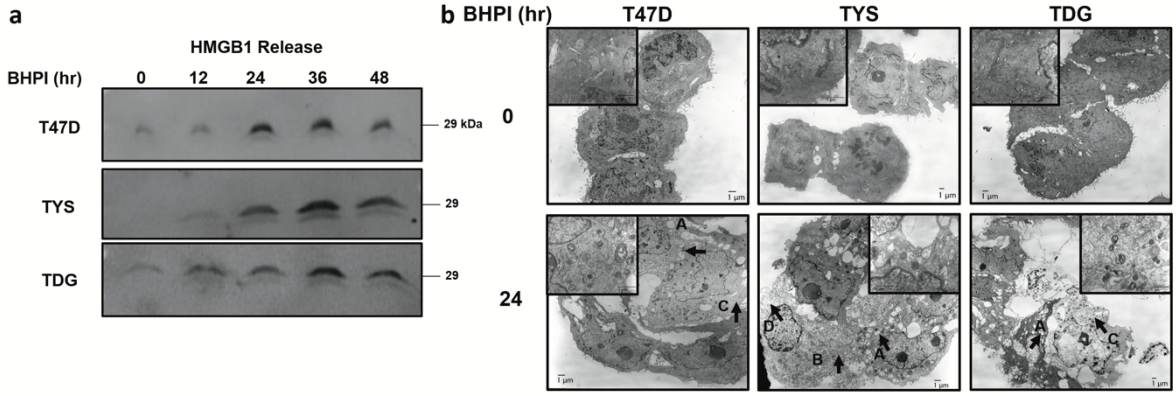

Figure 21. BHPI-induced cell death exhibits a necrotic phenotype. (a) Western blot analysis of HMGB1 release into the cell culture supernatant at the indicated time points from T47D, TYS, and TDG cells treated with 1 μM BHPI. Equal volumes of culture supernatant were loaded for analysis. (b) Transmission electron microscopy (TEM) images of T47D, TYS, and TDG cells treated with 1 μM BHPI for 0 or 24 hr. Letters with arrows indicate features characteristic of necrotic morphology: (A) swollen vacuoles, (B) swollen mitochondria, (C) cytoplasmic lightening (D) membrane rupture/"ghost" cells.

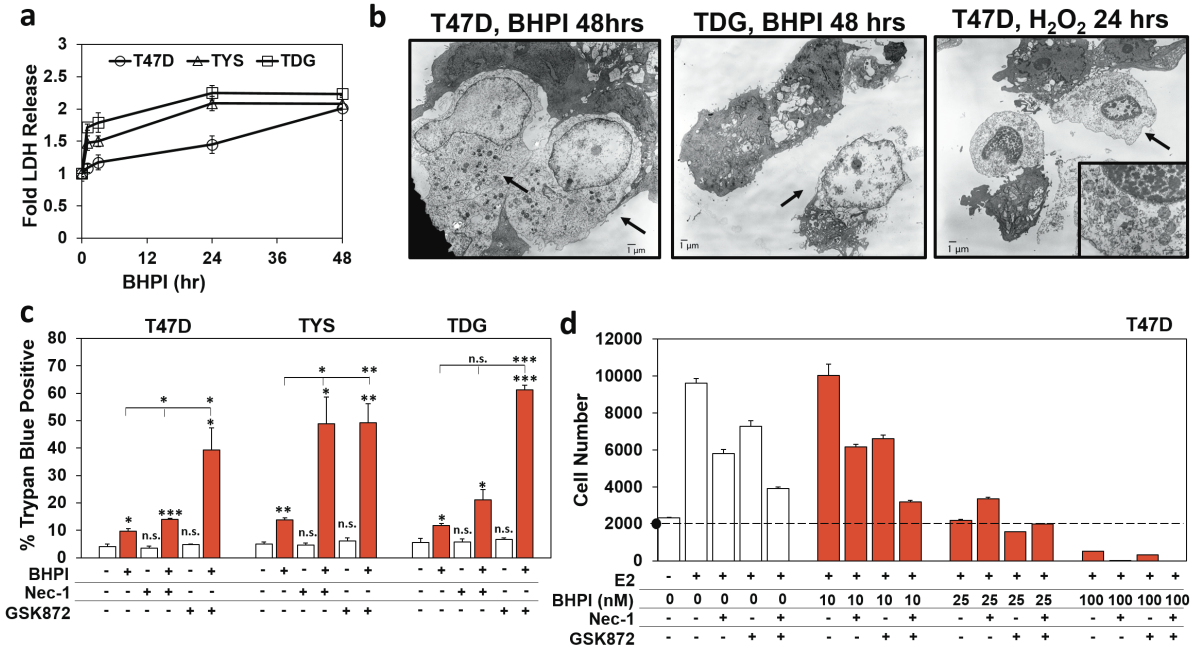

Figure 22. BHPI induces necrotic, but not necroptotic, cell death. (a) Lactate dehydrogenase (LDH) release into the cell culture supernatant at the indicated times after treatment of T47D, TYS, and TDG cells with 1 μM BHPI. Data is mean ± s.e.m (n=4 biological replicate experiments). (b) Transmission electron microscopy images of T47D and TDG cells treated with 1 μM BHPI for 48 hr, or T47D cells treated with 3 mM H_2O_2 for 24 hr. Arrows indicate cells that have lost membrane integrity and have leaked cytosolic contents to become "ghost" cells. (c) Trypan blue exclusion assays of T47D and TDG cells treated for 24 hr or TYS cells treated for 1 hr as indicated: BHPI 1 μM; Nec-1 100 μM; GSK872 5 μM. Data is mean ± s.e.m (n=3 biological replicate experiments), *p<0.05, **p<0.01, ***p<0.001, n.s. = not significant by Student's T-test. (d) T47D cell proliferation after 4 days treatment in 10% CD-calf serum with the indicated treatment: E_2 100 pM; 7-Cl-O-Nec-1 (Nec-1) 100 μM; GSK872 (GSK) 5 μM. Alamar-blue assay. Data is mean ± s.e.m (n=8 biological replicate experiments).

Necrotic Death Is an Early Outcome of Anticipatory UPR Hyperactivation and ATP Depletion Is Critical

BHPI-induced hyperactivation of the anticipatory UPR results in robust PERK activation and rapid, near-quantitative inhibition of protein synthesis at initiation.[29] The potent activator of eIF2B, ISRIB, reversed BHPI-induced inhibition of protein synthesis (Figure 23a).[137] At later times, BHPI also inhibits protein synthesis at elongation, through activation of AMPK and phosphorylation of eEF2; and ISRIB did not reverse inhibition of protein synthesis (Figure 24a).[29] While ISRIB

completely blocked BHPI-induced inhibition of protein synthesis, it did not block rapid necrotic death in TYS cells (Figure 23b).

We next asked if events upstream of PERK activation in the anticipatory UPR trigger necrosis, specifically, calcium release from IP_3Rs. Over several days, knockdown of some essential components of the anticipatory UPR, such as all three IP_3R calcium channel isoforms, results in substantial damage to cells. Moreover, the powerful IP_3R signal induced by hyperactivation of the anticipatory UPR could not be blocked by the IP_3 sponge, or by IP_3 phosphatase.[13,138] Notably, 2-APB completely blocked rapid cell death in TYS and MCF-7 cells (Figure 23c). Demonstrating PLCγ activation and IP_3 production are necessary for rapid cell death, siRNA knockdown of PLCγ nearly abolished BHPI-induced cell death (Figure 24b).

IP_3 binds to and opens IP_3 receptor (IP_3R) calcium channels causing a rapid and sustained release of calcium from the lumen of the EnR into the cytosol.[29,122] This creates an ATP-depleting futile cycle, where energy-dependent EnR SERCA pumps try to restore calcium homeostasis by pumping the calcium back into the lumen of the EnR, only to have it leak back out due to sustained opening of IP_3Rs.[29,122] Strikingly, the inhibitor of the SERCA pump, THG, significantly reduced rapid BHPI-induced cell death in TYS and MCF-7 cells (Figure 23d). We previously showed that in MCF-7 cells, THG blocks BHPI-induced ATP depletion.[29] Consistent with a critical role for ATP depletion in BHPI-induced necrotic death, BHPI caused significant ATP depletion in TYS cells within 1 hour that was blocked by THG (Figure 23e). We therefore compared the time course of BHPI-induced ATP depletion with the time course of cell death (note that the apparent increase in cell viability at 24 hours in TYS cells in Figure 23e is due to ~23% loss of disintegrated dead cells that are not visualized as trypan blue positive, we estimate viability to be 59%). Supporting

a central role for ATP depletion in cell death, the time course of the onset of necrotic cell death in T47D, TYS, and TDG cells is correlated with the onset of ATP depletion (Figure 23e).

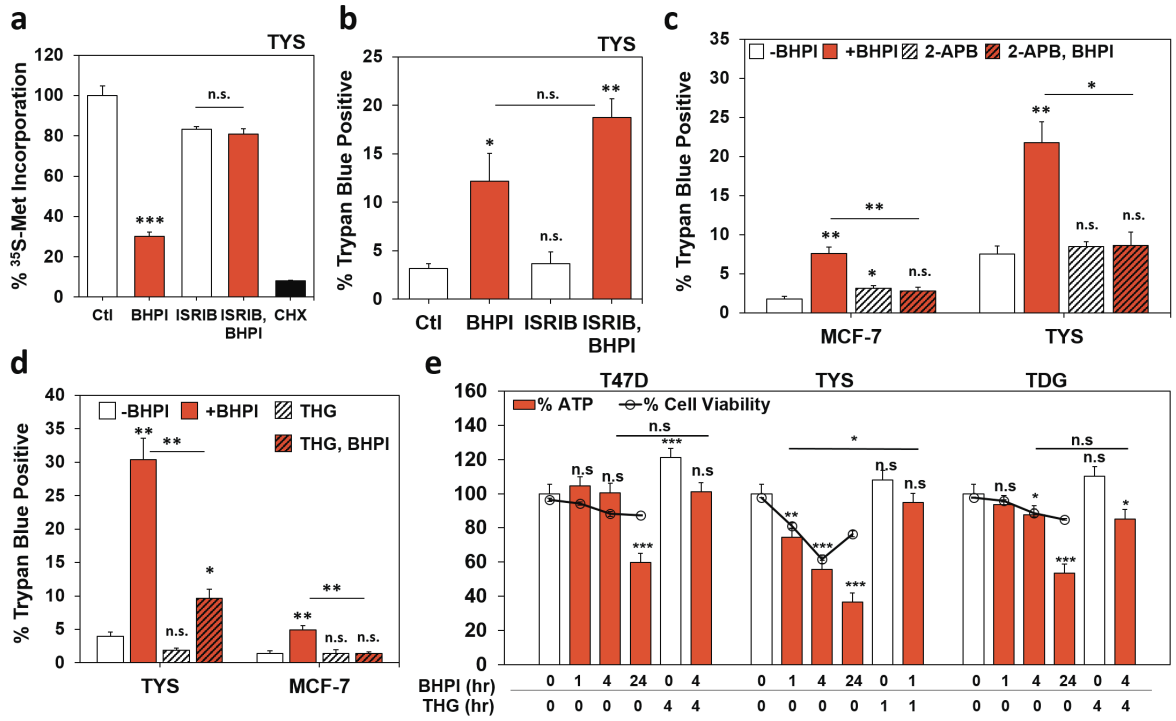

Figure 23. BHPI-induced necrosis is an upstream effect of anticipatory UPR activation and requires ATP depletion. (a) Incorporation of ^{35}S-methionine into newly synthesized protein in TYS cells treated for 1 hr with vehicle (set to 100%), 50 nM BHPI, 200 nM ISRIB, BHPI + ISRIB, or 10 µM cyclohexamide (CHX). (b) ISRIB does not prevent BHPI-induced cell death. Trypan blue exclusion assay for cell death in TYS cells after 1 hr treatment with vehicle, 1 µM BHPI, 200 nM ISRIB, or BHPI + ISRIB. (c) Locking the EnR IP_3R calcium channels closed with 2-APB blocks BHPI-induced cell death. Trypan blue exclusion assay for cell death in MCF-7 and TYS cells treated for 1 hr with vehicle, 1 µM BHPI, 100 µM 2-APB, or BHPI + 2-APB. (d) THG inhibits BHPI-induced cell death. Trypan blue exclusion assay for cell death in TYS and MCF-7 cells treated for 1 hr with vehicle, 1 µM BHPI, 10 µM THG, or BHPI + THG. (e) Time-dependent decline in ATP levels in BHPI-treated cells correlates with cell death. Measurement of whole-cell ATP levels (bars) and trypan blue exclusion (overlay, [o]) after treatment for the indicated times with vehicle, 1 µM BHPI, 10 µM THG, or BHPI + THG. For TYS cells, ~23% of cells have died at early times and disintegrated at 24 hr and are not counted by the instrument. Therefore, the percentage of trypan blue excluding cells declines at 24 hr, the total number of dead cells (trypan blue positive + disintegrated cells) is estimated to be ~59%. Data is mean ± s.e.m (a) (n=4 biological replicate experiments), (b-d) (n=3 biological replicate experiments), (e) (n=5 biological replicate experiments; ATP) (n=3 biological replicate experiments; cell viability) *p<0.05, **p<0.01, ***p<0.001, n.s. = not significant by Student's T-test.

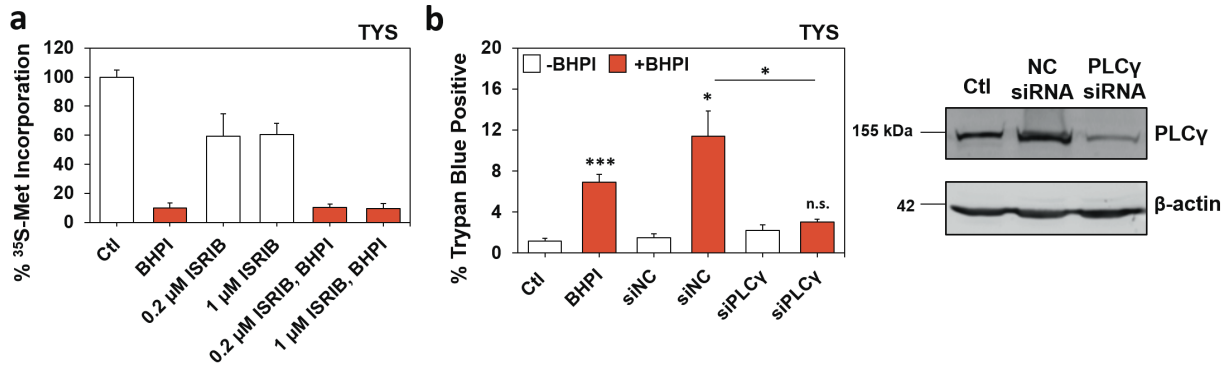

Figure 24. BHPI-induced necrosis requires activation of the anticipatory UPR through PLCγ. (a) Incorporation of ^{35}S-methionine into newly synthesized protein in TYS cells treated for 4 hr with vehicle, 50 nM BHPI, 0.2 or 1 μM ISRIB, or 0.2 or 1 μM ISRIB + 50 nM BHPI. Data is mean ± s.e.m (n=4 biological replicate experiments). (b) Trypan blue exclusion assay and western blot analysis of TYS cells. Cells were treated with 100 nM non-coding (siNC) or PLCγ (siPLCγ) siRNA for 16 hr. 48 hr following transfection, cells were treated with 50 nM BHPI for 2 hr before analysis. Data is mean ± s.e.m (n=3 biological replicate experiments) *p<0.05, **p<0.01, ***p<0.001, n.s. = not significant by Student's T-test.

Necrotic Products Released From BHPI-treated Cells Upregulate Inflammatory Markers and Increase Migration in THP-1 Cells

THP-1 cells are a commonly used human monocytic cell line that can be differentiated into macrophage. Using conditioned medium from T47D or TYS cells treated with vehicle or BHPI for 24 hours, we were able to show that necrotic products released from ERα$^+$ cancer cells caused induction of inflammatory mRNAs in THP-1 macrophage (Figure 25a) and increased migration in THP-1 monocytes (Figure 25b). Interestingly, conditioned medium from necrotic cells caused considerably more chemotaxis than conditioned medium from apoptotic cells (Figure 25b,c).

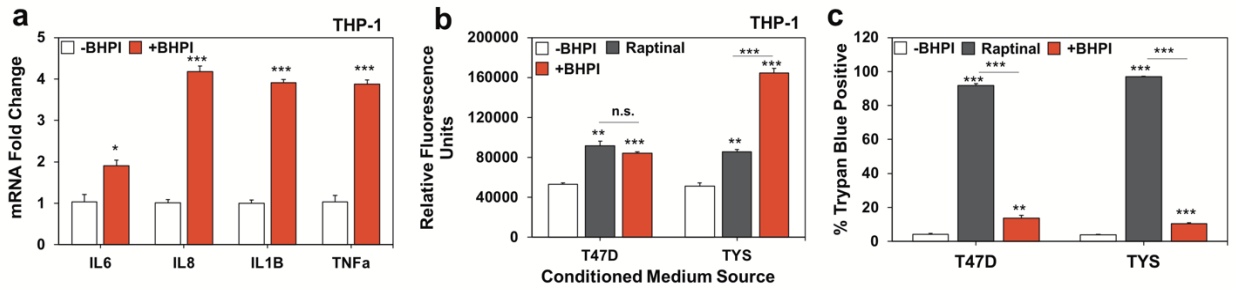

Figure 25. Conditioned medium from necrotic T47D and TYS cells causes an inflammatory response in THP-1 cells. (a) mRNA analysis of induction of inflammatory markers in THP-1 macrophage. Differentiated THP-1 cells were incubated for 6 hr with conditioned medium from TYS cells that had been treated with vehicle or 1 μM BHPI for 24 hr. (b) Fluorometric analysis of migration of THP-1 monocytes through a 5 μm filter. THP-1 cells were allowed to migrate for 4 hr towards conditioned medium from T47D or TYS cells that had been treated with vehicle, 10 μM Raptinal, or 1 μM BHPI for 24 hr. (c) Trypan blue exclusion assay of T47D and TYS cells treated with vehicle, 10 μM Raptinal, or 1 μM BHPI for 24 hr. Data is mean ± s.e.m (n=3 biological replicate experiments) *p<0.05, **p<0.01, ***p<0.001, n.s. = not significant by Student's T-test.

Discussion

Tumors must proliferate and overcome hypoxia, nutritional deprivation, and stress due to chemotherapy. In response, tumors activate the reactive UPR, which helps them overcome the stress, survive, and metastasize.[27] Activation of key UPR components, including BiP/GRP78/HSPA5 and XBP1, is implicated in development of diverse cancers including breast, lymphoma, lung, and glioma.[28] Although strong and sustained activation of the reactive UPR triggers caspase-dependent apoptosis, most drugs that target the reactive UPR usually work by inhibiting action of a UPR component and therefore must avoid toxicity in cells with a high secretory load.[35,52,105,106] An attractive alternative is targeting the anticipatory UPR that we, and others, showed is activated by the mitogenic hormones estrogen, progesterone, EGF, and VEGF.[12–14] Instead of inhibiting a component of this pathway, BHPI exploits the moderate activation of this protective pathway in ERα$^+$ cancer cells by hyperactivating the anticipatory UPR.[29] This pushes UPR activation in ERα$^+$ cancer cells into the lethal range. Thus, BHPI is both a promising

preclinical anticancer drug with a unique mode of action,[29,36] and a powerful tool for analyzing the death pathway induced by strong and sustained activation of the anticipatory UPR.

A unique feature of strong and sustained activation of the anticipatory UPR is rapid ATP depletion. Well-studied activators of the reactive UPR do not induce ATP depletion. Therefore, the consequences for cancer cell fate of BHPI-induced hyperactivation of the anticipatory UPR, sustained opening of IP_3R calcium channels, and subsequent ATP depletion were unclear.

We explored the relationships between three events triggered by BHPI treatment: rapid cell swelling, release of arachidonic acid, and cell death. A model depicting our findings is Figure 26. The most striking consequence of anticipatory UPR activation, disruption of calcium homeostasis, and ATP depletion is necrotic cell death.[56] Consistent with necrosis, we observed increased membrane permeability shown by leakage of intracellular proteins such as HMGB1 and LDH (Figures 21a and 22a). Furthermore, TEM images of T47D, TYS, and TDG cells treated with BHPI showed classical features of necrotic morphology including lysosomal and mitochondrial swelling and lightening of the cytoplasm (Figure 21b). At high concentrations, H_2O_2 induces disruption of calcium homeostasis, ATP depletion, and necrosis.[56,131,133,139] Consistent with BHPI inducing necrotic cell death, BHPI and H_2O_2-treated cells exhibited similar morphology. Notably, after 24 hours in TYS cells or 48 hours in T47D and TDG cells, we observed a "ghost" cell population exhibiting severely disintegrated membranes and massive leakage of intracellular contents (Figures 21b, and 22b).

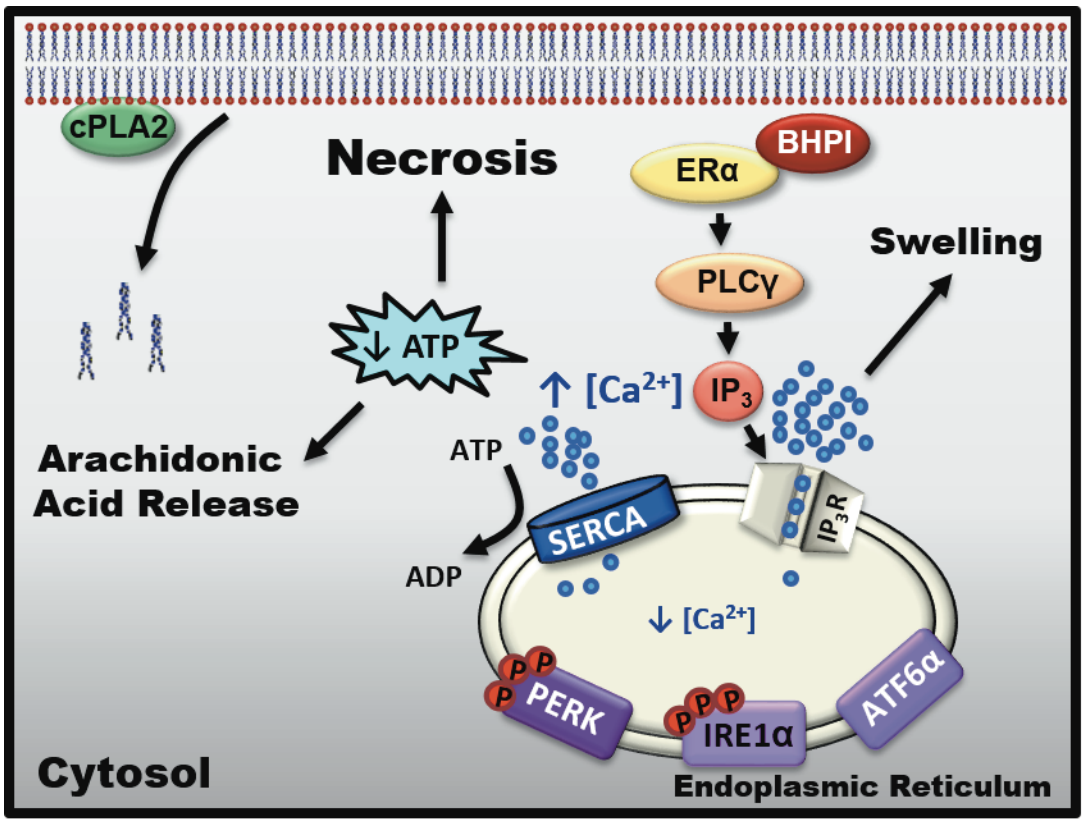

Figure 26. Model depicting events that follow BHPI hyperactivation of the anticipatory UPR. UPR hyperactivation triggers three parallel events: cell swelling, arachidonic acid release, and necrotic cell death. Activation of PLCγ leads to production of IP_3. Opening of IP_3R calcium channels in the endoplasmic reticulum results in efflux of calcium from the lumen of the endoplasmic reticulum into the cell body. This calcium release is necessary for cell swelling. Pumping of cytosol calcium back into the lumen of the endoplasmic reticulum, by ATP-dependent SERCA pumps, and calcium leaking back out through the open IP_3Rs causes an ATP-depleting futile cycle necessary for both arachidonic acid release and necrotic cell death.

Cytosolic calcium overload, such as is seen with BHPI-opening of EnR IP_3R calcium channels, is implicated in both apoptosis and necrosis.[39] Demonstrating calcium release from IP_3Rs is necessary for cell death, 2-APB completely blocked rapid death in TYS and MCF-7 cells (Figure 23c). Prolonged activation of the reactive UPR results in apoptotic cell death. However, near-quantitative inhibition of protein synthesis by BHPI blocks production of pro-apoptotic UPR mediators, such as CHOP (Figure 14e). Interestingly, we also observed inhibition of autophagy upon BHPI treatment (Figure 16). It is possible that the reduced requirement for amino acids due

to near quantitative inhibition of protein synthesis by BHPI is linked to inhibition of autophagy. Inhibiting autophagy, may exacerbate BHPI-induced UPR activation and ATP depletion, and consequently, necrotic cell death.

Programmed cell death by apoptosis and autophagy require ATP; activation of caspase-9 in the apoptosome and phagophore elongation are ATP-dependent.[55] When ATP is depleted, cells fail to initiate apoptosis and/or autophagy, and necrotic cell death is induced.[39] Commonly, necrotic ATP depletion is caused by mitochondrial dysfunction after disruption of calcium homeostasis.[140] In contrast, BHPI indirectly activates SERCA pumps, causing cells to consume ATP faster than they produce it, a mechanism reminiscent of PARP-mediated ATP depletion after excessive DNA damage.[131] We analyzed the role of ATP depletion using THG, which inhibits ATP-dependent SERCA pumps in the EnR and reverses BHPI-mediated ATP depletion.[29] Consistent with loss of ATP playing a pivotal role in activating necrotic cell death, and despite inducing an increase in intracellular calcium similar to that seen with BHPI,[29] THG potently reversed rapid death in TYS and MCF-7 cells (Figure 23d). Since THG is lethal over time,[51] we could not test the effect of THG on T47D and TDG cells. Supporting a role for ATP depletion in necrotic cell death following sustained activation of the anticipatory UPR, death and ATP depletion were correlated in T47D, TYS, and TDG cells (Figure 23e). Notably, in TYS cells, but not in T47D and TDG cells, BHPI induces both a decline in ATP levels and cell viability in 1 hour.

Within 1 hour and prior to cell death, BHPI caused ERα-mediated, time and concentration-dependent cell swelling (Figures 17a,b and 18a-c). Cell swelling is associated with and is commonly a precursor to necrosis.[121] Swelling was specific to BHPI's unique mechanism of action and required ERα, opening of EnR IP_3R calcium channels, intracellular calcium, and extracellular ions (Figure 18d,f). Weak anticipatory UPR activators, reactive UPR activators, endocrine

therapies, and chemotherapeutic drugs did not cause cell swelling (Figure 17c-e). Notably, blocking BHPI-mediated ATP depletion with THG did not inhibit rapid swelling (Figure 20c), but did block death (Figure 23d).

In contrast, ATP depletion was required for cPLA2 activation as THG blocked AA release from membranes (Figure 19c). While assaying ATP levels in the entire T47D cell at 1 hour did not show ATP depletion, it is possible that local ATP levels at membranes are reduced. Interestingly, while calcium activates cPLA2,[123–125] THG, which increases intracellular calcium but does not reduce ATP levels, did not induce AA release. Instead, THG blocked BHPI-mediated AA release (Figure 19c). Additionally, even though both THG and the cPLA2 inhibitor Quin block AA release from cells, only Quin blocked cell swelling (Figure 19d). Within cells, AA can be converted to pro-inflammatory prostaglandins by COX (cyclooxygenase).[128,129] We saw a modest, not statistically significant, increase in prostaglandins in the medium from BHPI-treated cells. Together, BHPI-mediated release of AA metabolites, and necrotic leakage of immunomodulatory proteins such as HMGB1, might create an inflammatory tumor environment conducive to increased immune detection and killing of tumor cells *in vivo*.[142,143] Preliminary data from THP-1 cells indicates that the small molecules and proteins released from BHPI-treated necrotic cells are sufficient to activate macrophage and monocytes *in vitro* (Figure 25).

While we found that rapid cell swelling, AA release, and cell death are linked to early steps in sustained activation of the anticipatory UPR and require calcium release from IP_3Rs, they are parallel and distinct results. Notably, ATP depletion independently activates cPLA2 and triggers necrotic cell death. This work demonstrates that in contrast to reactive UPR activators that kill cells through CHOP-mediated apoptosis, BHPI, a small-molecule activator of the anticipatory UPR, kills cells through necrosis. Importantly, ATP depletion is the critical cause of necrotic cell

death after strong and sustained activation of the anticipatory UPR. Thus, we show that different modes of UPR activation trigger different death pathways.

CHAPTER 5: DISCUSSION

It was previously unknown if BHPI could effectively target T47D breast cancer cells expressing the constitutively active mutations ERαY537S (TYS cells) and ERαD538G (TDG cells). In 3D culture, OHT and fulvestrant/ICI only partially inhibited growth of TYS and TDG cells and R5020 completely reversed antiestrogen inhibition of growth. This resistance is consistent with recent studies and with data suggesting patients carrying metastatic tumors with these mutations have a poor prognosis.[40,45] Additionally, TYS and TDG cells express higher levels of the molecular chaperones BiP and $p58^{IPK}$ and P_4 further elevates some of these downstream products of mild UPR activation. Elevated expression of UPR components is known to be associated with cancer progression,[30,31] and specifically, BiP is protective and contributes to antiestrogen resistance.[144] In contrast to the antiestrogens, BHPI not only blocked the growth of, but killed TYS and TDG cells in the presence or absence of R5020. Since BHPI is not a competitive inhibitor of ERα and targets ERα positive cancer cells irrespective of their dependence on E_2 for proliferation, it is a promising preclinical drug candidate for the treatment of metastatic breast cancers expressing these mutations. Moreover, BHPI qualitatively appears to target and kill TYS and TDG cells better than T47D cells expressing wildtype ERα. While yet untested, it is possible that the further mild and protective upregulation of the anticipatory UPR in TYS and TDG cells makes them more vulnerable to hyperactivation of the UPR by BHPI, and subsequent cell death. This idea is consistent with our finding that up-regulation of a UPR gene index in ERα positive breast cancer patients is tightly correlated with tamoxifen resistance, reduced time to recurrence, and a poor prognosis.[14]

Since BHPI effectively kills breast and endometrial cancer cell lines, including TYS and TDG cells, our next aim was to identify the cell death pathway it activates. Unlike most small molecules

that activate the classical reactive UPR, BHPI does not kill cells through CHOP and caspase-dependent apoptosis. There is no evidence of caspase activation in the mechanism of cell death, and the cell morphology does not match shrinking and blebbing apoptotic cells. Additionally, BHPI does not activate, but rather seems to inhibit autophagy. Surprisingly, BHPI hyperactivation of the anticipatory UPR leads to necrotic cell death. We confirmed necrotic cell death morphology by observation of cell swelling, vacuolization and swelling of organelles, and eventual membrane rupture of T47D, TYS, and TDG cells, and by monitoring the release of cytosolic contents. Necrotic cell death is induced by disruption of calcium homeostasis through production of IP_3 and opening of EnR IP_3R channels, followed by an ATP-depleting futile cycle as energy-dependent SERCA pumps try to restore calcium homeostasis. Interestingly, rapid and dramatic ATP depletion is the critical step to initiate necrotic cell death. This was the first time that the death pathway induced by hyperactivation of the anticipatory UPR was described.

Given this mechanism of action of BHPI, we were curios to ask what the consequences of necrotic cell death induced by hyperactivation of the anticipatory UPR might be on the immune system. In an effort to increase immune responses to tumor antigens, recent goals of anti-cancer drug development include targeting immune checkpoints, identification of drugs that activate immunogenic cell death (ICD), and engineering oncolytic cancer vaccines.[142,143,145] Of note, while necrotic cells produced through freeze-thaw cycles are not immunogenic, cells that have undergone necrosis after chemical modification with oxidizing agents or small molecules have shown exceptional potential.[143] For example, necroptotic cancer cells effectively activate immune cells and vaccinate mice against a future tumor challenge.[146] Despite intense interest in this area, necrotic cell death, caused by hyperactivation of the anticipatory UPR has never before been linked to activation of inflammatory signaling in immune cells.

In addition to the release of AA from cancer cells, BHPI killing of cells through necrosis allows the release of a host of immunomodulatory small molecules and proteins including ATP, HMGB1, heat shock proteins, and IL-1α. These molecules are known to alter the activation, cytokine production, and migration potential of a variety of immune cells including monocytes, macrophage, and dendritic cells.[147–150] Once activated, these cells can then go on to activate lymphoid cells, such as T cells, that target and help eliminate the cancer cells. While necrotic products released from T47D and TYS cells treated with BHPI activated THP-1 monocytes and macrophage, it is currently unclear what contribution the various necrotic products, including small molecules and proteins, make to this inflammatory response. In the future, it will also be important to understand how a coordinated and complex immune system recognizes and responds to a necrotic tumor *in vivo*.

After therapy, most ERα$^+$ breast cancers go into remission. However, after many years, some cancers recur at the site of origin or as metastatic breast cancer due to residual or disseminated tumor cells. Metastatic cancers harboring mutations in ERα, including ERαY537S and ERαD538G, that recur are often resistant to classical endocrine therapy. It is thought that after treatment, and possibly up to 5 years preceding relapse, these cancerous cells lie dormant. Immunosurveilance has long been thought to play a role in encouraging dormancy of cancers.[151,152] It is therefore interesting to ask the following questions. First, will the necrotic cell death induced by BHPI activate an immune response *in vivo*? I have shown that BHPI effectively targets and kills endocrine therapy resistant cancer cells expressing ERαY537S and ERαD538G. Therefore, could BHPI treatment lead to a robust immune response that might completely wipe out every last cancer cell not effectively targeted by BHPI, especially those cancers that have developed resistance to classical therapies? And if not, could the potential immune response induced by BHPI

lead to production of cells, such as memory T cells, that could keep the residual cancer cells in a dormant state indefinitely?

BHPI is a unique small molecule with a novel mechanism of action, as it was the first molecule identified to induce necrotic cell death by hyperactivating the anticipatory UPR through ERα. Not only does it target diverse ERα$^+$ breast, endometrial, and ovarian cancer cells, but it also effectively eliminates many ERα$^+$ cancer cells that are resistant to current endocrine therapies, including those expressing mutations in the ERα LBD.[15,29,153,154] Importantly, BHPI may recapitulate elements of immunotherapy in a small molecule, thereby synergizing with its potent ability to shrink tumors in our immunocompromised mouse model,[29,46] and increasing its efficacy *in vivo*.

REFERENCES

1 Ron D, Walter P. Signal integration in the endoplasmic reticulum unfolded protein response. *Nat Rev Mol Cell Biol* 2007; **8**: 519–529.

2 Walter P, Ron D. The unfolded protein response: from stress pathway to homeostatic regulation. *Science* 2011; **334**: 1081–1086.

3 Urra H, Dufey E, Avril T, Chevet E, Hetz C. Endoplasmic Reticulum Stress and the Hallmarks of Cancer. *Trends Cancer* 2016; **2**: 252–262.

4 Korennykh A, Walter P. Structural basis of the unfolded protein response. *Annu Rev Cell Dev Biol* 2012; **28**: 251–277.

5 Preissler S, Chambers JE, Crespillo-Casado A, Avezov E, Miranda E, Perez J *et al.* Physiological modulation of BiP activity by trans-protomer engagement of the interdomain linker. *eLife* 2015; **4**: e08961.

6 Volmer R, Ron D. Lipid-dependent regulation of the unfolded protein response. *Curr Opin Cell Biol* 2015; **33**: 67–73.

7 Cox JS, Walter P. A novel mechanism for regulating activity of a transcription factor that controls the unfolded protein response. *Cell* 1996; **87**: 391–404.

8 Yoshida H, Haze K, Yanagi H, Yura T, Mori K. Identification of the cis-acting endoplasmic reticulum stress response element responsible for transcriptional induction of mammalian glucose-regulated proteins. Involvement of basic leucine zipper transcription factors. *J Biol Chem* 1998; **273**: 33741–33749.

9 Novoa I, Zeng H, Harding HP, Ron D. Feedback Inhibition of the Unfolded Protein Response by GADD34-Mediated Dephosphorylation of eIF2α. *J Cell Biol* 2001; **153**: 1011–1022.

10 van Anken E, Romijn EP, Maggioni C, Mezghrani A, Sitia R, Braakman I *et al.* Sequential Waves of Functionally Related Proteins Are Expressed When B Cells Prepare for Antibody Secretion. *Immunity* 2003; **18**: 243–253.

11 Hu C-CA, Dougan SK, McGehee AM, Love JC, Ploegh HL. XBP-1 regulates signal transduction, transcription factors and bone marrow colonization in B cells. *EMBO J* 2009; **28**: 1624–1636.

12 Karali E, Bellou S, Stellas D, Klinakis A, Murphy C, Fotsis T. VEGF Signals through ATF6 and PERK to promote endothelial cell survival and angiogenesis in the absence of ER stress. *Mol Cell* 2014; **54**: 559–572.

13 Yu L, Andruska N, Zheng X, Shapiro DJ. Anticipatory activation of the unfolded protein response by epidermal growth factor is required for immediate early gene expression and cell proliferation. *Mol Cell Endocrinol* 2016; **422**: 31–41.

14 Andruska N, Zheng X, Yang X, Helferich WG, Shapiro DJ. Anticipatory estrogen activation of the unfolded protein response is linked to cell proliferation and poor survival in estrogen receptor α-positive breast cancer. *Oncogene* 2015; **34**: 3760–3769.

15 Mao C, Livezey M, Kim JE, Shapiro DJ. Antiestrogen Resistant Cell Lines Expressing Estrogen Receptor α Mutations Upregulate the Unfolded Protein Response and are Killed by BHPI. *Sci Rep* 2016; **6**: 34753.

16 Liu W, Cai M-J, Zheng C-C, Wang J-X, Zhao X-F. Phospholipase Cγ1 Connects the Cell Membrane Pathway to the Nuclear Receptor Pathway in Insect Steroid Hormone Signaling. *J Biol Chem* 2014; **289**: 13026–13041.

17 Normanno N, De Luca A, Bianco C, Strizzi L, Mancino M, Maiello MR *et al.* Epidermal growth factor receptor (EGFR) signaling in cancer. *Gene* 2006; **366**: 2–16.
18 Deroo BJ, Korach KS. Estrogen receptors and human disease. *J Clin Invest* 2006; **116**: 561–570.
19 Evans RM. The steroid and thyroid hormone receptor superfamily. *Science* 1988; **240**: 889–895.
20 Huang P, Chandra V, Rastinejad F. Structural overview of the nuclear receptor superfamily: insights into physiology and therapeutics. *Annu Rev Physiol* 2010; **72**: 247–272.
21 Katzenellenbogen BS. Dynamics of steroid hormone receptor action. *Annu Rev Physiol* 1980; **42**: 17–35.
22 York B, O'Malley BW. Steroid receptor coactivator (SRC) family: masters of systems biology. *J Biol Chem* 2010; **285**: 38743–38750.
23 Carroll JS, Liu XS, Brodsky AS, Li W, Meyer CA, Szary AJ *et al.* Chromosome-wide mapping of estrogen receptor binding reveals long-range regulation requiring the forkhead protein FoxA1. *Cell* 2005; **122**: 33–43.
24 Hah N, Danko CG, Core L, Waterfall JJ, Siepel A, Lis JT *et al.* A rapid, extensive, and transient transcriptional response to estrogen signaling in breast cancer cells. *Cell* 2011; **145**: 622–634.
25 Levin ER. Plasma membrane estrogen receptors. *Trends Endocrinol Metab TEM* 2009; **20**: 477–482.
26 Song RX-D, Santen RJ. Membrane initiated estrogen signaling in breast cancer. *Biol Reprod* 2006; **75**: 9–16.
27 Ma Y, Hendershot LM. The role of the unfolded protein response in tumour development: friend or foe? *Nat Rev Cancer* 2004; **4**: 966–977.
28 Wang M, Kaufman RJ. The impact of the endoplasmic reticulum protein-folding environment on cancer development. *Nat Rev Cancer* 2014; **14**: 581–597.
29 Andruska ND, Zheng X, Yang X, Mao C, Cherian MM, Mahapatra L *et al.* Estrogen receptor α inhibitor activates the unfolded protein response, blocks protein synthesis, and induces tumor regression. *Proc Natl Acad Sci* 2015; **112**: 4737–4742.
30 Chen X, Iliopoulos D, Zhang Q, Tang Q, Greenblatt MB, Hatziapostolou M *et al.* XBP1 promotes triple-negative breast cancer by controlling the HIF1α pathway. *Nature* 2014; **508**: 103–107.
31 Zhao N, Cao J, Xu L, Tang Q, Dobrolecki LE, Lv X *et al.* Pharmacological targeting of MYC-regulated IRE1/XBP1 pathway suppresses MYC-driven breast cancer. *J Clin Invest* 2018; **128**: 1283–1299.
32 Wang M, Kaufman RJ. Protein misfolding in the endoplasmic reticulum as a conduit to human disease. *Nature* 2016; **529**: 326–335.
33 Clarke R, Cook KL, Hu R, Facey COB, Tavassoly I, Schwartz JL *et al.* Endoplasmic reticulum stress, the unfolded protein response, autophagy, and the integrated regulation of breast cancer cell fate. *Cancer Res* 2012; **72**: 1321–1331.
34 Rajapaksa G, Thomas C, Gustafsson J-Å. Estrogen signaling and unfolded protein response in breast cancer. *J Steroid Biochem Mol Biol* 2016; **163**: 45–50.
35 Sykes EK, Mactier S, Christopherson RI. Melanoma and the Unfolded Protein Response. *Cancers* 2016; **8**. doi:10.3390/cancers8030030.

36 Zheng X, Andruska N, Lambrecht MJ, He S, Parissenti A, Hergenrother PJ *et al.* Targeting multidrug-resistant ovarian cancer through estrogen receptor α dependent ATP depletion caused by hyperactivation of the unfolded protein response. *Oncotarget* 2018; **9**: 14741–14753.
37 Berridge MJ, Bootman MD, Roderick HL. Calcium signalling: dynamics, homeostasis and remodelling. *Nat Rev Mol Cell Biol* 2003; **4**: 517–529.
38 Criddle DN, Gerasimenko JV, Baumgartner HK, Jaffar M, Voronina S, Sutton R *et al.* Calcium signalling and pancreatic cell death: apoptosis or necrosis? *Cell Death Differ* 2007; **14**: 1285–1294.
39 Bruce JIE. Metabolic regulation of the PMCA: Role in cell death and survival. *Cell Calcium* 2018; **69**: 28–36.
40 Robinson DR, Wu Y-M, Vats P, Su F, Lonigro RJ, Cao X *et al.* Activating ESR1 mutations in hormone-resistant metastatic breast cancer. *Nat Genet* 2013; **45**: 1446–1451.
41 Toy W, Shen Y, Won H, Green B, Sakr RA, Will M *et al.* ESR1 ligand-binding domain mutations in hormone-resistant breast cancer. *Nat Genet* 2013; **45**: 1439–1445.
42 Spoerke JM, Gendreau S, Walter K, Qiu J, Wilson TR, Savage H *et al.* Heterogeneity and clinical significance of ESR1 mutations in ER-positive metastatic breast cancer patients receiving fulvestrant. *Nat Commun* 2016; **7**: 11579.
43 Fanning SW, Mayne CG, Dharmarajan V, Carlson KE, Martin TA, Novick SJ *et al.* Estrogen receptor alpha somatic mutations Y537S and D538G confer breast cancer endocrine resistance by stabilizing the activating function-2 binding conformation. *eLife* 2016; **5**. doi:10.7554/eLife.12792.
44 Merenbakh-Lamin K, Ben-Baruch N, Yeheskel A, Dvir A, Soussan-Gutman L, Jeselsohn R *et al.* D538G Mutation in Estrogen Receptor-α: A Novel Mechanism for Acquired Endocrine Resistance in Breast Cancer. *Cancer Res* 2013; **73**: 6856–6864.
45 Chandarlapaty S, Chen D, He W, Sung P, Samoila A, You D *et al.* Prevalence of ESR1 Mutations in Cell-Free DNA and Outcomes in Metastatic Breast Cancer: A Secondary Analysis of the BOLERO-2 Clinical Trial. *JAMA Oncol* 2016; **2**: 1310–1315.
46 Zhao Y, Laws MJ, Guillen VS, Ziegler Y, Min J, Sharma A *et al.* Structurally Novel Antiestrogens Elicit Differential Responses from Constitutively Active Mutant Estrogen Receptors in Breast Cancer Cells and Tumors. *Cancer Res* 2017; **77**: 5602–5613.
47 Weir HM, Bradbury RH, Lawson M, Rabow AA, Buttar D, Callis RJ *et al.* AZD9496: An Oral Estrogen Receptor Inhibitor That Blocks the Growth of ER-Positive and ESR1-Mutant Breast Tumors in Preclinical Models. *Cancer Res* 2016; **76**: 3307–3318.
48 Xiong R, Zhao J, Gutgesell LM, Wang Y, Lee S, Karumudi B *et al.* Novel Selective Estrogen Receptor Downregulators (SERDs) Developed against Treatment-Resistant Breast Cancer. *J Med Chem* 2017; **60**: 1325–1342.
49 Bihani T, Patel HK, Arlt H, Tao N, Jiang H, Brown JL *et al.* Elacestrant (RAD1901), a Selective Estrogen Receptor Degrader (SERD), Has Antitumor Activity in Multiple ER+Breast Cancer Patient-derived Xenograft Models. *Clin Cancer Res Off J Am Assoc Cancer Res* 2017; **23**: 4793–4804.
50 Onuki R, Bando Y, Suyama E, Katayama T, Kawasaki H, Baba T *et al.* An RNA-dependent protein kinase is involved in tunicamycin-induced apoptosis and Alzheimer's disease. *EMBO J* 2004; **23**: 959–968.
51 Yamaguchi H, Bhalla K, Wang H-G. Bax plays a pivotal role in thapsigargin-induced apoptosis of human colon cancer HCT116 cells by controlling Smac/Diablo and Omi/HtrA2 release from mitochondria. *Cancer Res* 2003; **63**: 1483–1489.

52 Nawrocki ST, Carew JS, Pino MS, Highshaw RA, Dunner K, Huang P *et al.* Bortezomib sensitizes pancreatic cancer cells to endoplasmic reticulum stress-mediated apoptosis. *Cancer Res* 2005; **65**: 11658–11666.
53 McCullough KD, Martindale JL, Klotz L-O, Aw T-Y, Holbrook NJ. Gadd153 Sensitizes Cells to Endoplasmic Reticulum Stress by Down-Regulating Bcl2 and Perturbing the Cellular Redox State. *Mol Cell Biol* 2001; **21**: 1249–1259.
54 Elmore S. Apoptosis: A Review of Programmed Cell Death. *Toxicol Pathol* 2007; **35**: 495–516.
55 Maiuri MC, Zalckvar E, Kimchi A, Kroemer G. Self-eating and self-killing: crosstalk between autophagy and apoptosis. *Nat Rev Mol Cell Biol* 2007; **8**: 741–752.
56 Golstein P, Kroemer G. Cell death by necrosis: towards a molecular definition. *Trends Biochem Sci* 2007; **32**: 37–43.
57 Andruska N, Mao C, Cherian M, Zhang C, Shapiro DJ. Evaluation of a luciferase-based reporter assay as a screen for inhibitors of estrogen-ERα-induced proliferation of breast cancer cells. *J Biomol Screen* 2012; **17**: 921–932.
58 Ran FA, Hsu PD, Wright J, Agarwala V, Scott DA, Zhang F. Genome engineering using the CRISPR-Cas9 system. *Nat Protoc* 2013; **8**: 2281–2308.
59 Ke N, Albers A, Claassen G, Yu D, Chatterton JE, Hu X *et al.* One-week 96-well soft agar growth assay for cancer target validation. *BioTechniques* 2004; **36**: 826–828, 830, 832–833.
60 Zhang QX, Borg A, Wolf DM, Oesterreich S, Fuqua SA. An estrogen receptor mutant with strong hormone-independent activity from a metastatic breast cancer. *Cancer Res* 1997; **57**: 1244–1249.
61 Fribbens C, O'Leary B, Kilburn L, Hrebien S, Garcia-Murillas I, Beaney M *et al.* Plasma ESR1 Mutations and the Treatment of Estrogen Receptor-Positive Advanced Breast Cancer. *J Clin Oncol Off J Am Soc Clin Oncol* 2016. doi:10.1200/JCO.2016.67.3061.
62 Schiavon G, Hrebien S, Garcia-Murillas I, Cutts RJ, Pearson A, Tarazona N *et al.* Analysis of ESR1 mutation in circulating tumor DNA demonstrates evolution during therapy for metastatic breast cancer. *Sci Transl Med* 2015; **7**: 313ra182.
63 Yu M, Bardia A, Aceto N, Bersani F, Madden MW, Donaldson MC *et al.* Ex vivo culture of circulating breast tumor cells for individualized testing of drug susceptibility. *Science* 2014; **345**: 216–220.
64 Paoletti C, Larios JM, Muñiz MC, Aung K, Cannell EM, Darga EP *et al.* Heterogeneous estrogen receptor expression in circulating tumor cells suggests diverse mechanisms of fulvestrant resistance. *Mol Oncol* 2016; **10**: 1078–1085.
65 Weis KE, Ekena K, Thomas JA, Lazennec G, Katzenellenbogen BS. Constitutively active human estrogen receptors containing amino acid substitutions for tyrosine 537 in the receptor protein. *Mol Endocrinol* 1996; **10**: 1388–1398.
66 Stender JD, Frasor J, Komm B, Chang KCN, Kraus WL, Katzenellenbogen BS. Estrogen-regulated gene networks in human breast cancer cells: involvement of E2F1 in the regulation of cell proliferation. *Mol Endocrinol Baltim Md* 2007; **21**: 2112–2123.
67 Doudna JA, Charpentier E. Genome editing. The new frontier of genome engineering with CRISPR-Cas9. *Science* 2014; **346**: 1258096.
68 Smith C, Abalde-Atristain L, He C, Brodsky BR, Braunstein EM, Chaudhari P *et al.* Efficient and allele-specific genome editing of disease loci in human iPSCs. *Mol Ther J Am Soc Gene Ther* 2015; **23**: 570–577.

69 Maruyama T, Dougan SK, Truttmann MC, Bilate AM, Ingram JR, Ploegh HL. Increasing the efficiency of precise genome editing with CRISPR-Cas9 by inhibition of nonhomologous end joining. *Nat Biotechnol* 2015; **33**: 538–542.
70 Chu VT, Weber T, Wefers B, Wurst W, Sander S, Rajewsky K *et al.* Increasing the efficiency of homology-directed repair for CRISPR-Cas9-induced precise gene editing in mammalian cells. *Nat Biotechnol* 2015; **33**: 543–548.
71 Richardson CD, Ray GJ, DeWitt MA, Curie GL, Corn JE. Enhancing homology-directed genome editing by catalytically active and inactive CRISPR-Cas9 using asymmetric donor DNA. *Nat Biotechnol* 2016; **34**: 339–344.
72 Diep CH, Daniel AR, Mauro LJ, Knutson TP, Lange CA. Progesterone action in breast, uterine, and ovarian cancers. *J Mol Endocrinol* 2015; **54**: R31–R53.
73 Obr AE, Edwards DP. The biology of progesterone receptor in the normal mammary gland and in breast cancer. *Mol Cell Endocrinol* 2012; **357**: 4–17.
74 Mohammed H, Russell IA, Stark R, Rueda OM, Hickey TE, Tarulli GA *et al.* Progesterone receptor modulates ERα action in breast cancer. *Nature* 2015; **523**: 313–317.
75 Kytölä S, Rummukainen J, Nordgren A, Karhu R, Farnebo F, Isola J *et al.* Chromosomal alterations in 15 breast cancer cell lines by comparative genomic hybridization and spectral karyotyping. *Genes Chromosomes Cancer* 2000; **28**: 308–317.
76 Mao C, Patterson NM, Cherian MT, Aninye IO, Zhang C, Montoya JB *et al.* A New Small Molecule Inhibitor of Estrogen Receptor α Binding to Estrogen Response Elements Blocks Estrogen-dependent Growth of Cancer Cells. *J Biol Chem* 2008; **283**: 12819–12830.
77 Obrero M, Yu DV, Shapiro DJ. Estrogen Receptor-dependent and Estrogen Receptor-independent Pathways for Tamoxifen and 4-Hydroxytamoxifen-induced Programmed Cell Death. *J Biol Chem* 2002; **277**: 45695–45703.
78 Zhou J-H, Yu DV, Cheng J, Shapiro DJ. Delayed and persistent ERK1/2 activation is required for 4-hydroxytamoxifen-induced cell death. *Steroids* 2007; **72**: 765–777.
79 Zheng X, Andruska N, Yu L, Mao C, Kim JE, Livezey M *et al.* Interplay between steroid hormone activation of the unfolded protein response and nuclear receptor action. *Steroids* 2016. doi:10.1016/j.steroids.2016.03.014.
80 Shapiro DJ, Livezey M, Yu L, Zheng X, Andruska N. Anticipatory UPR Activation: A Protective Pathway and Target in Cancer. *Trends Endocrinol Metab TEM* 2016; **27**: 731–741.
81 Lee AS. GRP78 Induction in Cancer: Therapeutic and Prognostic Implications. *Cancer Res* 2007; **67**: 3496–3499.
82 Zhang J, Jiang Y, Jia Z, Li Q, Gong W, Wang L *et al.* Association of elevated GRP78 expression with increased lymph node metastasis and poor prognosis in patients with gastric cancer. *Clin Exp Metastasis* 2006; **23**: 401–410.
83 Gao D, Bambang IF, Putti TC, Lee YK, Richardson DR, Zhang D. ERp29 induces breast cancer cell growth arrest and survival through modulation of activation of p38 and upregulation of ER stress protein p58IPK. *Lab Investig J Tech Methods Pathol* 2012; **92**: 200–213.
84 May D, Itin A, Gal O, Kalinski H, Feinstein E, Keshet E. Ero1-L alpha plays a key role in a HIF-1-mediated pathway to improve disulfide bond formation and VEGF secretion under hypoxia: implication for cancer. *Oncogene* 2005; **24**: 1011–1020.
85 Jiang Y, Zhang W, Kondo K, Klco JM, St Martin TB, Dufault MR *et al.* Gene expression profiling in a renal cell carcinoma cell line: dissecting VHL and hypoxia-dependent pathways. *Mol Cancer Res MCR* 2003; **1**: 453–462.

86 Hsu PD, Lander ES, Zhang F. Development and Applications of CRISPR-Cas9 for Genome Engineering. *Cell* 2014; **157**: 1262–1278.
87 Wu Y, Liang D, Wang Y, Bai M, Tang W, Bao S *et al.* Correction of a Genetic Disease in Mouse via Use of CRISPR-Cas9. *Cell Stem Cell* 2013; **13**: 659–662.
88 Schwank G, Koo B-K, Sasselli V, Dekkers JF, Heo I, Demircan T *et al.* Functional Repair of CFTR by CRISPR/Cas9 in Intestinal Stem Cell Organoids of Cystic Fibrosis Patients. *Cell Stem Cell* 2013; **13**: 653–658.
89 Wang H, Yang H, Shivalila CS, Dawlaty MM, Cheng AW, Zhang F *et al.* One-Step Generation of Mice Carrying Mutations in Multiple Genes by CRISPR/Cas-Mediated Genome Engineering. *Cell* 2013; **153**: 910–918.
90 Niu Y, Shen B, Cui Y, Chen Y, Wang J, Wang L *et al.* Generation of Gene-Modified Cynomolgus Monkey via Cas9/RNA-Mediated Gene Targeting in One-Cell Embryos. *Cell* 2014; **156**: 836–843.
91 Liang P, Xu Y, Zhang X, Ding C, Huang R, Zhang Z *et al.* CRISPR/Cas9-mediated gene editing in human tripronuclear zygotes. *Protein Cell* 2015; **6**: 363–372.
92 Zheng Q, Cai X, Tan MH, Schaffert S, Arnold CP, Gong X *et al.* Precise gene deletion and replacement using the CRISPR/Cas9 system in human cells. *BioTechniques* 2014; **57**: 115–124.
93 Cradick TJ, Fine EJ, Antico CJ, Bao G. CRISPR/Cas9 systems targeting β-globin and CCR5 genes have substantial off-target activity. *Nucleic Acids Res* 2013; **41**: 9584–9592.
94 Cho SW, Kim S, Kim Y, Kweon J, Kim HS, Bae S *et al.* Analysis of off-target effects of CRISPR/Cas-derived RNA-guided endonucleases and nickases. *Genome Res* 2014; **24**: 132–141.
95 Fu Y, Foden JA, Khayter C, Maeder ML, Reyon D, Joung JK *et al.* High-frequency off-target mutagenesis induced by CRISPR-Cas nucleases in human cells. *Nat Biotechnol* 2013; **31**: 822–826.
96 Hasty P, Rivera-Pérez J, Bradley A. The length of homology required for gene targeting in embryonic stem cells. *Mol Cell Biol* 1991; **11**: 5586–5591.
97 McCormack P, Sapunar F. Pharmacokinetic profile of the fulvestrant loading dose regimen in postmenopausal women with hormone receptor-positive advanced breast cancer. *Clin Breast Cancer* 2008; **8**: 347–351.
98 Croxtall JD, McKeage K. Fulvestrant: a review of its use in the management of hormone receptor-positive metastatic breast cancer in postmenopausal women. *Drugs* 2011; **71**: 363–380.
99 Jeselsohn R, Yelensky R, Buchwalter G, Frampton G, Meric-Bernstam F, Gonzalez-Angulo AM *et al.* Emergence of constitutively active estrogen receptor-α mutations in pretreated advanced estrogen receptor-positive breast cancer. *Clin Cancer Res Off J Am Assoc Cancer Res* 2014; **20**: 1757–1767.
100 Ladd B, Mazzola AM, Bihani T, Lai Z, Bradford J, Collins M *et al.* Effective combination therapies in preclinical endocrine resistant breast cancer models harboring ER mutations. *Oncotarget* 2016. doi:10.18632/oncotarget.10852.
101 Li S, Shen D, Shao J, Crowder R, Liu W, Prat A *et al.* Endocrine-therapy-resistant ESR1 variants revealed by genomic characterization of breast-cancer-derived xenografts. *Cell Rep* 2013; **4**: 1116–1130.
102 Sunar F, Gormus ZI, Baltaci AK, Mogulkoc R. The effect of low dose zinc supplementation to serum estrogen and progesterone levels in post-menopausal women. *Biol Trace Elem Res* 2008; **126 Suppl 1**: S11-14.

103 Lucisano A, Acampora MG, Russo N, Maniccia E, Montemurro A, Dell'Acqua S. Ovarian and peripheral plasma levels of progestogens, androgens and oestrogens in post-menopausal women. *Maturitas* 1984; **6**: 45–53.
104 Yoo KY, Kim H, Shin HR, Kang D, Ha M, Park SK *et al.* Female sex hormones and body mass in adolescent and postmenopausal Korean women. *J Korean Med Sci* 1998; **13**: 241–246.
105 Hensel F, Eckstein M, Rosenwald A, Brändlein S. Early development of PAT-SM6 for the treatment of melanoma. *Melanoma Res* 2013; **23**: 264–275.
106 Fasano E, Serini S, Piccioni E, Toesca A, Monego G, Cittadini AR *et al.* DHA induces apoptosis by altering the expression and cellular location of GRP78 in colon cancer cell lines. *Biochim Biophys Acta* 2012; **1822**: 1762–1772.
107 Wright TM, Wardell SE, Jasper JS, Stice JP, Safi R, Nelson ER *et al.* Delineation of a FOXA1/ERα/AGR2 regulatory loop that is dysregulated in endocrine therapy-resistant breast cancer. *Mol Cancer Res MCR* 2014; **12**: 1829–1839.
108 Sano R, Reed JC. ER stress-induced cell death mechanisms. *Biochim Biophys Acta* 2013; **1833**: 3460–3470.
109 Devarajan E, Sahin AA, Chen JS, Krishnamurthy RR, Aggarwal N, Brun A-M *et al.* Down-regulation of caspase 3 in breast cancer: a possible mechanism for chemoresistance. *Oncogene* 2002; **21**: 8843–8851.
110 Mooney LM, Al-Sakkaf KA, Brown BL, Dobson PRM. Apoptotic mechanisms in T47D and MCF-7 human breast cancer cells. *Br J Cancer* 2002; **87**: 909–917.
111 Zhang Y, Zhang B. TRAIL resistance of breast cancer cells is associated with constitutive endocytosis of death receptors 4 and 5. *Mol Cancer Res MCR* 2008; **6**: 1861–1871.
112 Kim I, Xu W, Reed JC. Cell death and endoplasmic reticulum stress: disease relevance and therapeutic opportunities. *Nat Rev Drug Discov* 2008; **7**: 1013–1030.
113 Nishitoh H. CHOP is a multifunctional transcription factor in the ER stress response. *J Biochem (Tokyo)* 2012; **151**: 217–219.
114 Oyadomari S, Mori M. Roles of CHOP/GADD153 in endoplasmic reticulum stress. *Cell Death Differ* 2004; **11**: 381–389.
115 Kaur J, Debnath J. Autophagy at the crossroads of catabolism and anabolism. *Nat Rev Mol Cell Biol* 2015; **16**: 461–472.
116 Ogata M, Hino S, Saito A, Morikawa K, Kondo S, Kanemoto S *et al.* Autophagy is activated for cell survival after endoplasmic reticulum stress. *Mol Cell Biol* 2006; **26**: 9220–9231.
117 Deegan S, Saveljeva S, Logue SE, Pakos-Zebrucka K, Gupta S, Vandenabeele P *et al.* Deficiency in the mitochondrial apoptotic pathway reveals the toxic potential of autophagy under ER stress conditions. *Autophagy* 2014; **10**: 1921–1936.
118 Kang R, Zeh HJ, Lotze MT, Tang D. The Beclin 1 network regulates autophagy and apoptosis. *Cell Death Differ* 2011; **18**: 571–580.
119 Mizushima N, Komatsu M. Autophagy: renovation of cells and tissues. *Cell* 2011; **147**: 728–741.
120 Jewell JL, Russell RC, Guan K-L. Amino acid signalling upstream of mTOR. *Nat Rev Mol Cell Biol* 2013; **14**: 133–139.
121 Majno G, Joris I. Apoptosis, oncosis, and necrosis. An overview of cell death. *Am J Pathol* 1995; **146**: 3–15.
122 Zheng X, Andruska N, Lambrecht MJ, He S, Parissenti A, Hergenrother PJ *et al.* Targeting multidrug-resistant ovarian cancer through estrogen receptor α dependent ATP depletion caused

by hyperactivation of the unfolded protein response. *Oncotarget* 2017; **5**. doi:10.18632/oncotarget.10819.
123 Mouchlis VD, Dennis EA. Membrane and inhibitor interactions of intracellular phospholipases A2. *Adv Biol Regul* 2016; **61**: 17–24.
124 Burke JE, Dennis EA. Phospholipase A2 structure/function, mechanism, and signaling. *J Lipid Res* 2009; **50**: S237–S242.
125 Enyedi B, Jelcic M, Niethammer P. The Cell Nucleus Serves as a Mechanotransducer of Tissue Damage-Induced Inflammation. *Cell* 2016; **165**: 1160–1170.
126 Lang F, Busch GL, Ritter M, Völkl H, Waldegger S, Gulbins E *et al.* Functional significance of cell volume regulatory mechanisms. *Physiol Rev* 1998; **78**: 247–306.
127 Staub F, Winkler A, Peters J, Kempski O, Kachel V, Baethmann A. Swelling, acidosis, and irreversible damage of glial cells from exposure to arachidonic acid in vitro. *J Cereb Blood Flow Metab Off J Int Soc Cereb Blood Flow Metab* 1994; **14**: 1030–1039.
128 Miller SB. Prostaglandins in health and disease: an overview. *Semin Arthritis Rheum* 2006; **36**: 37–49.
129 Gilroy DW, Newson J, Sawmynaden P, Willoughby DA, Croxtall JD. A novel role for phospholipase A2 isoforms in the checkpoint control of acute inflammation. *FASEB J Off Publ Fed Am Soc Exp Biol* 2004; **18**: 489–498.
130 Leist M, Single B, Castoldi AF, Kühnle S, Nicotera P. Intracellular adenosine triphosphate (ATP) concentration: a switch in the decision between apoptosis and necrosis. *J Exp Med* 1997; **185**: 1481–1486.
131 Zong W-X, Ditsworth D, Bauer DE, Wang Z-Q, Thompson CB. Alkylating DNA damage stimulates a regulated form of necrotic cell death. *Genes Dev* 2004; **18**: 1272–1282.
132 Krysko DV, Vanden Berghe T, Parthoens E, D'Herde K, Vandenabeele P. Methods for distinguishing apoptotic from necrotic cells and measuring their clearance. *Methods Enzymol* 2008; **442**: 307–341.
133 McKeague AL, Wilson DJ, Nelson J. Staurosporine-induced apoptosis and hydrogen peroxide-induced necrosis in two human breast cell lines. *Br J Cancer* 2003; **88**: 125–131.
134 Cai Z, Liu Z-G. Execution of RIPK3-regulated necrosis. *Mol Cell Oncol* 2014; **1**. doi:10.4161/23723548.2014.960759.
135 Vandenabeele P, Grootjans S, Callewaert N, Takahashi N. Necrostatin-1 blocks both RIPK1 and IDO: consequences for the study of cell death in experimental disease models. *Cell Death Differ* 2013; **20**: 185–187.
136 Mandal P, Berger SB, Pillay S, Moriwaki K, Huang C, Guo H *et al.* RIP3 induces apoptosis independent of pronecrotic kinase activity. *Mol Cell* 2014; **56**: 481–495.
137 Sidrauski C, Tsai JC, Kampmann M, Hearn BR, Vedantham P, Jaishankar P *et al.* Pharmacological dimerization and activation of the exchange factor eIF2B antagonizes the integrated stress response. *eLife* 2015; **4**: e07314.
138 Hernandez CC, Zaika O, Tolstykh GP, Shapiro MS. Regulation of neural KCNQ channels: signalling pathways, structural motifs and functional implications. *J Physiol* 2008; **586**: 1811–1821.
139 Castro J, Bittner CX, Humeres A, Montecinos VP, Vera JC, Barros LF. A cytosolic source of calcium unveiled by hydrogen peroxide with relevance for epithelial cell death. *Cell Death Differ* 2004; **11**: 468–478.
140 Vanlangenakker N, Vanden Berghe T, Krysko DV, Festjens N, Vandenabeele P. Molecular mechanisms and pathophysiology of necrotic cell death. *Curr Mol Med* 2008; **8**: 207–220.

142 Workenhe ST, Mossman KL. Oncolytic virotherapy and immunogenic cancer cell death: sharpening the sword for improved cancer treatment strategies. *Mol Ther J Am Soc Gene Ther* 2014; **22**: 251–256.
143 Vandenberk L, Belmans J, Van Woensel M, Riva M, Van Gool SW. Exploiting the Immunogenic Potential of Cancer Cells for Improved Dendritic Cell Vaccines. *Front Immunol* 2015; **6**: 663.
144 Fu Y, Li J, Lee AS. GRP78/BiP Inhibits Endoplasmic Reticulum BIK and Protects Human Breast Cancer Cells against Estrogen Starvation–Induced Apoptosis. *Cancer Res* 2007; **67**: 3734–3740.
145 Postow MA, Callahan MK, Wolchok JD. Immune Checkpoint Blockade in Cancer Therapy. *J Clin Oncol Off J Am Soc Clin Oncol* 2015; **33**: 1974–1982.
146 Aaes TL, Kaczmarek A, Delvaeye T, De Craene B, De Koker S, Heyndrickx L *et al.* Vaccination with Necroptotic Cancer Cells Induces Efficient Anti-tumor Immunity. *Cell Rep* 2016; **15**: 274–287.
147 El Mezayen R, El Gazzar M, Seeds MC, McCall CE, Dreskin SC, Nicolls MR. Endogenous signals released from necrotic cells augment inflammatory responses to bacterial endotoxin. *Immunol Lett* 2007; **111**: 36–44.
148 Müller S, Scaffidi P, Degryse B, Bonaldi T, Ronfani L, Agresti A *et al.* The double life of HMGB1 chromatin protein: architectural factor and extracellular signal. *EMBO J* 2001; **20**: 4337–4340.
149 Paolo NCD, Shayakhmetov DM. Interleukin 1α and the inflammatory process. *Nat Immunol* 2016; **17**: 906–913.
150 Ashida N, Arai H, Yamasaki M, Kita T. Distinct Signaling Pathways for MCP-1-dependent Integrin Activation and Chemotaxis. *J Biol Chem* 2001; **276**: 16555–16560.
151 Aguirre-Ghiso JA. Models, mechanisms and clinical evidence for cancer dormancy. *Nat Rev Cancer* 2007; **7**: 834–846.
152 Sosa MS, Bragado P, Aguirre-Ghiso JA. Mechanisms of disseminated cancer cell dormancy: an awakening field. *Nat Rev Cancer* 2014; **14**: 611–622.
153 Livezey M, Huang R, Hergenrother PJ, Shapiro DJ. Strong and sustained activation of the anticipatory unfolded protein response induces necrotic cell death. *Cell Death Differ* 2018. doi:10.1038/s41418-018-0143-2.
154 Livezey M, Kim JE, Shapiro DJ. A New Role for Estrogen Receptor α in Cell Proliferation and Cancer: Activating the Anticipatory Unfolded Protein Response. *Front Endocrinol* 2018; **9**. doi:10.3389/fendo.2018.00325.